A BDDC ALGORITHM WITH DELUXE SCALING FOR H(CURL) IN TWO DIMENSIONS WITH IRREGULAR SUBDOMAINS

JUAN G. CALVO *

TR2014-965

Abstract. A bound is obtained for the condition number of a BDDC algorithm for problems posed in $H(\mathrm{curl})$ in two dimensions, where the subdomains are only assumed to be uniform in the sense of Peter Jones. For the primal variable space, a continuity constraint for the tangential average over each interior subdomain edge is imposed. For the averaging operator, a new technique named deluxe scaling is used. Our bound is independent of jumps in the coefficients across the interface between the subdomains and depends only on a few geometric parameters of the decomposition. Numerical results that verify the result are shown, including some with subdomains with fractal edges and others obtained by a mesh partitioner.

Key words. domain decomposition, BDDC preconditioner, irregular subdomain boundaries, H(curl), Maxwell's equations, discontinuous coefficients, preconditioners

AMS subject classifications. 35Q60, 65F10, 65N30, 65N55

1. Introduction.

We consider the boundary value problem in two dimensions (2D)

$$\nabla \times (\alpha \nabla \times \boldsymbol{u}) + B\boldsymbol{u} = \boldsymbol{f} \text{ in } \Omega, \tag{1.1a}$$

$$\boldsymbol{u} \times \boldsymbol{n} = 0 \text{ on } \partial\Omega, \tag{1.1b}$$

where $\alpha(\boldsymbol{x}) \geq 0$, B is a 2×2 strictly positive definite symmetric matrix and Ω a uniform domain; see [17] and Section 4. These domains form the largest family for which a bounded extension of $H(\mathrm{grad}, \Omega)$ to $H(\mathrm{grad}, \mathbb{R}^2)$ is possible, where $H(\mathrm{grad}, \Omega)$ is the subspace of $L^2(\Omega)$ with a finite L^2-norm of its gradient. They were introduced as (ϵ, δ) domains in [17] and we will consider the case $\delta = \infty$. We could equally well consider cases where the boundary condition (1.1b) is imposed only on one or several subdomain edges which form part of $\partial\Omega$, imposing a natural boundary condition over the rest of the boundary.

In order to formulate an appropriate weak form for this problem, we consider the Hilbert space $H(\mathrm{curl}, \Omega)$, the subspace of $(L^2(\Omega))^2$ with a finite L^2-norm of its curl. We then obtain a weak formulation for (1.1): Find $\boldsymbol{u} \in H_0(\mathrm{curl}, \Omega)$ such that

$$a(\boldsymbol{u}, \boldsymbol{v}) = (\boldsymbol{f}, \boldsymbol{v}) \qquad \forall \boldsymbol{v} \in H_0(\mathrm{curl}, \Omega), \tag{1.2}$$

with

$$a(\boldsymbol{u}, \boldsymbol{v}) := \int_\Omega [\alpha(\nabla \times \boldsymbol{u})(\nabla \times \boldsymbol{v}) + B\boldsymbol{u} \cdot \boldsymbol{v}]\, d\boldsymbol{x}, \qquad (\boldsymbol{f}, \boldsymbol{v}) := \int_\Omega \boldsymbol{f} \cdot \boldsymbol{v} d\boldsymbol{x}. \tag{1.3}$$

Here, $H_0(\mathrm{curl}, \Omega)$ is the subspace of $H(\mathrm{curl}, \Omega)$ with a vanishing tangential component on $\partial\Omega$. The norm of $\boldsymbol{u} \in H(\mathrm{curl}, \Omega)$, for a domain with diameter 1, is given by $a(\boldsymbol{u}, \boldsymbol{u})^{1/2}$ with $\alpha = 1$ and $B = I$. The problem (1.2) arises, for example, from implicit time integration of the eddy current model of Maxwell's equation; see [2, Chapter 8]. It is also considered in [1, 31, 36, 16].

We decompose the domain Ω into N non-overlapping subdomains $\{\Omega_i\}_{i=1}^N$, which are uniform in the sense of Jones [17] and each of which is the union of elements of the triangulation $\mathcal{T}_h$ of Ω. Each Ω_i is simply connected and has a connected boundary $\partial\Omega_i$. We denote by H_i the diameter of Ω_i, by h_i the smallest element diameter of the shape-regular triangulation $\mathcal{T}_{h_i}$ of Ω_i and by H/h the maximum of the ratios H_i/h_i.

*Courant Institute of Mathematical Sciences, 251 Mercer Street, New York, NY 10012, USA `calvo@cims.nyu.edu` This work was supported in part by the National Science Foundation Grant DMS-1216564 and in part by the U.S. Department of Energy under contracts DE-FG02-06ER25718.

The main purpose of this paper is to construct and analyze a BDDC (Balancing Domain Decomposition by Constraints) preconditioner for the problem (1.2) discretized with Nédélec finite elements (introduced in [25]) in two dimensions and for irregular subdomains. The condition number estimate will be given in terms of a few simple geometric parameters of the subdomains Ω_i.

The BDDC method was first proposed in [6]. Convergence bounds for these algorithms were provided in [8]. The BDDC methods are closely related to the dual-primal finite element tearing and interconnecting methods (FETI-DP): the spectra of the relevant operators of these two algorithms are the same, except possibly for eigenvalues of 0 and 1, for the same set of primal constraints; see, e.g., [9, 23].

In the construction of a BDDC preconditioner, a set of primal constraints and a weighted average need to be chosen and these choices affect the rate of convergence. For the primal variable space, we impose a continuity constraint for the tangential average over each subdomain edge; see Section 2 for more details.

Classical choices for the weighted average include the inverse of the cardinality of a subdomain edge (the number of subdomains sharing the edge) and weights proportional to entries on the diagonals of subdomain matrices. Also, in [32] a scaling that depends on the coefficients α and β is considered, but with the limitation that only one coefficient is allowed to present discontinuities. We will use a deluxe average, introduced in [12] for three dimensional problems. This technique is used in [5], where a BDDC preconditioner is extended to Isogeometric Analysis for scalar elliptic problems. The bound is independent of coefficients discontinuities across the interface. This deluxe average is also used in [21, 27, 13].

In domain decomposition theory, it is typically assumed that each subdomain is quite regular, e.g., the union of a small set of coarse triangles or tetrahedra. But, it is unrealistic in general to assume that each subdomain is regular. Thus, subdomain boundaries that arise from mesh partitioners might not even be Lipschitz continuous, i.e., the number of patches required to cover the boundary of the region in each of which the boundary is the graph of a Lipschitz continuous function, might not be uniformly bounded independently of the finite element mesh size. Some recent work and technical tools have been developed for irregular subdomains, cf. [37]. Scalar elliptic problems in the plane are analyzed in [7, 10]; [19] includes a FETI-DP algorithm for scalar elliptic and elasticity problems, and [11] includes an iterative substructuring method for problems in $H(\text{curl})$ in 2D.

Some studies based on FETI algorithms for problem (1.2) include [20, 33] for problems posed in 2D, and [32] in 3D. The subdomains are bounded convex polyhedra and the bounds depend on the coefficients α_i, β_i and H_i.

In a previous study related to $H(\text{curl})$, the estimate $\kappa \leq C(1 + H/\delta)^2$ is given in [31] for an overlapping Schwarz algorithm in three dimensions, where the coarse space consists of standard edge finite element functions for coarse tetrahedral elements, the domain is assumed convex and $\alpha \equiv 1$, $B \equiv I$ over the whole domain. The coarse triangulation is shape-regular and quasi-uniform. Here, δ measures the overlap of the decomposition.

Work on vector valued problems also include [15], where overlapping Schwarz methods are analyzed for vector valued elliptic problems in $H(\text{curl})$ and $H(\text{div})$ in three dimensions. With the assumption of a convex polyhedral domain and $B = I$, the condition number is bounded by $C(1 + H/\delta)^2$, where subdomains are tetrahedra and constant coefficients are considered.

In [26], a two-level overlapping Schwarz method for Raviart-Thomas vector fields is developed. Here the bilinear form is

$$a(\boldsymbol{u}, \boldsymbol{v}) = \int_\Omega \alpha \text{div}\boldsymbol{u}\text{div}\boldsymbol{v} + \beta \boldsymbol{u} \cdot \boldsymbol{v} dx,$$

and the condition number is bounded by $C(1 + H/\delta)(1 + \log(H/h))$, where the domain is a bounded polyhedron in $\mathbb{R}^3$ and discontinuous coefficients and hexahedral elements are considered. A BDDC algorithm with deluxe averaging is studied in [27] for the space $H(\text{div})$, with Raviart-Thomas elements, where convex polyhedral subdomains are assumed. The condition number is bounded by $C(1+\log(H/h))^2$, where the constant is independent of the values and jumps of the coefficients across the interface.

An iterative substructuring method for problem (1.2) is analyzed in [36], where the bound $C(1+\log(H/h))^2$ is found for bounded polygonal domains in $\mathbb{R}^2$. The same bound is established in [35] for problems in $H(\text{div})$ under similar assumptions in $\mathbb{R}^3$. An iterative substructuring method for 2D problems is analyzed in [11] for irregular subdomains, where the condition number of the preconditioned operator is bounded by $C\chi^2(1+\log(H/h))^2$; see Lemma 5.10 for the definition of χ. We will borrow some technical tools derived in that paper. In addition, a BDDC algorithm in 3D is considered in [12, 13], where a deluxe scaling is considered.

Our study applies to a broad range of material properties and subdomain geometries. We obtain the optimal bound

$$\kappa \leq C\chi^2|\Xi|\left(1+\log\frac{H}{h}\right)^2$$

for our deluxe BDDC method, a bound independent of the jumps of the coefficients between the subdomains. We recall that condition number estimates obtained in previous studies depend on the coefficients of the problem. The constant χ is related to the geometry of the subdomains and it is quite small even for fractal edges and large values of H/h, and $|\Xi|$ represents the maximum number of neighbors for any subdomain.

The rest of this paper is organized as follows. In Section 2, we introduce the notation used. In Section 3, we present the BDDC methods and in Section 4 we introduce the definition of uniform domains and some related lemmas. Section 5 includes some technical tools that are used to prove our estimate of the condition number in Section 6. In Section 7, we report on some numerical experiments which confirm our theoretical result.

2. Notation. We introduce some notation that we will use throughout this paper. The interface of the decomposition $\{\Omega_i\}_{i=1}^N$ is given by

$$\Gamma := \left(\bigcup_{i=1}^{N}\partial\Omega_i\right)\setminus\partial\Omega,$$

and the contribution to Γ from $\partial\Omega_i$ by $\Gamma_i := \partial\Omega_i \setminus \partial\Omega$. These sets are unions of subdomain edges and vertices. We denote the subdomain edges of Ω_i by $\mathcal{E}^{ij} := \overline{\Omega}_i \cap \overline{\Omega}_j$, excluding the two vertices at its endpoints. We note that the intersection of the closure of two subdomains might have several components; in such a case, each component will be regarded as an edge. We will write $\mathcal{E}$ instead of $\mathcal{E}^{ij}$ when there is no ambiguity.

The set of all subdomain edges is defined as

$$S_{\mathcal{E}} := \{\mathcal{E}^{ij} : i < j, \mathcal{E}^{ij} \neq \emptyset\}$$

and $S_{\mathcal{E}_i}$ is the subset of subdomain edges which belong to Γ_i. When there is a need to uniquely define the unit tangential vector $\boldsymbol{t}_{\mathcal{E}}$ over a subdomain edge, we will select the subdomain with the smallest index and use the counterclockwise direction over the boundary of the relevant subdomain. The unit vector in the direction from one endpoint of a subdomain edge $\mathcal{E}$ to the other (with the same sense of direction as $\boldsymbol{t}_{\mathcal{E}}$) is denoted by $\boldsymbol{d}_{\mathcal{E}}$. The distance between the two endpoints is $d_{\mathcal{E}}$.

For any irregular subdomain edge $\mathcal{E}$, we will consider a covering by disks and we will denote by $\chi_{\mathcal{E}}(d)(d_{\mathcal{E}}/d)$ the number of closed circular disks of diameter d that are required to cover it. We note that $\chi_{\mathcal{E}}(d) = 1$ if the edge is straight. It can be proved that for a prefractal Koch snowflake curve, which is a polygon with side length h_i and diameter H_i, $\chi_{\mathcal{E}}(h_i) \leq (H_i/h_i)^{\log(4/3)} < (H_i/h_i)^{1/8}$; see [11, Section 3.2]. This is not a large factor, being less than 10 even in the extreme case of $H_i/h_i = 10^8$.

Associated with the triangulation $\mathcal{T}_{h_i}$, we consider the space of continuous, piecewise linear triangular nodal elements $W_{\text{grad}}^{h_i}(\Omega_i) \subset H(\text{grad},\Omega_i)$, and the space $W_{\text{curl}}^{h_i}(\Omega_i) \subset$

$H(\mathrm{curl}, \Omega_i)$, based on linear triangular Nédélec edge elements on Ω_i with zero tangential component on $\partial\Omega \cap \partial\Omega_i$; see [25].

The Nédélec elements are conforming in $H(\mathrm{curl}, \Omega)$ and those of lowest order are defined by

$$W^h_{\mathrm{curl}}(\Omega) := \{\boldsymbol{u} | \boldsymbol{u}_{|K} \in \mathcal{N}_1(K), K \in \mathcal{T}_h \text{ and } \boldsymbol{u} \in H(\mathrm{curl}, \Omega)\},$$

where any function in $\mathcal{N}_1(K)$ has the form $\boldsymbol{u}(x_1, x_2) = (a_1 + bx_2, a_2 - bx_1)^T$, with a_1, a_2, b real numbers. The degrees of freedom for an element $K \in \mathcal{T}_h$ are given by the average values of the tangential component over the edges of the elements, i.e.,

$$\lambda_e(\boldsymbol{u}) := \frac{1}{|e|} \int_e \boldsymbol{u} \cdot \boldsymbol{t}_e ds, \tag{2.1}$$

with $e \in \partial K$ and $\boldsymbol{t}_e$ a unit vector in the direction of e. We recall that a function in $W^h_{\mathrm{curl}}(\Omega)$ has a continuous tangential component across all the fine edges; see e.g. [25].

We replace B by βI, and assume that α, β are constants α_i, β_i in each subdomain Ω_i. We denote by $a_i(\boldsymbol{u}, \boldsymbol{v})$ the bilinear form $a(\cdot, \cdot)$ defined in (1.3) restricted to Ω_i, and by $E_D(\boldsymbol{v})$ the energy of $\boldsymbol{v}$ over the set D, i.e.

$$E_D(\boldsymbol{v}) := \int_D \alpha |\nabla \times \boldsymbol{v}|^2 + \beta |\boldsymbol{v}|^2 dx.$$

For simplicity, we write $W^{(i)} := W^{h_i}_{\mathrm{curl}}(\Omega_i)$. We decompose this space into two, $W^{(i)} := W^{(i)}_I \oplus W^{(i)}_\Gamma$, where $W^{(i)}_I$ represents the interior space and $W^{(i)}_\Gamma$ the interface space, associated to the interior and interface degrees of freedom, respectively. We decompose the space $W^{(i)}_\Gamma$ as the sum of a dual and a primal space, $W^{(i)}_\Gamma := W^{(i)}_\Delta \oplus W^{(i)}_\Pi$.

For $\mathcal{E} \in S_\mathcal{E}$, we define the coarse function $\boldsymbol{c}_\mathcal{E}$ with tangential data given by $\boldsymbol{c}_\mathcal{E} \cdot \boldsymbol{t}_\mathcal{E} = \boldsymbol{d}_\mathcal{E} \cdot \boldsymbol{t}_\mathcal{E}$ along $\mathcal{E}$ and with $\boldsymbol{c}_\mathcal{E} \cdot \boldsymbol{t}_\mathcal{E} = 0$ on $\Gamma \cup \partial\Omega \setminus \mathcal{E}$. Then $\boldsymbol{c}_\mathcal{E}$ is fully defined by the energy minimizing extension of this tangential data into the interior of the two subdomains sharing $\mathcal{E}$. This set of coarse functions was introduced in [11, Section 2].

The primal space will be spanned by these coarse basis functions, and therefore its dimension is the same as the number of interior subdomain edges. For each subdomain, given $\boldsymbol{u}^{(i)} \in W^{(i)}$, we define

$$\boldsymbol{u}^{(i)}_\Pi := \sum_{\mathcal{E} \in S_{\mathcal{E}_i}} \bar{u}_\mathcal{E} \boldsymbol{c}_\mathcal{E}, \text{ with } \bar{u}_\mathcal{E} := \frac{1}{d_\mathcal{E}} \int_\mathcal{E} \boldsymbol{u}^{(i)} \cdot \boldsymbol{t}_\mathcal{E} ds. \tag{2.2}$$

In other words, given $\boldsymbol{u}^{(i)} \in W^{(i)}$ and $\boldsymbol{u}^{(j)} \in W^{(j)}$, we impose the constraint

$$\int_{\mathcal{E}^{ij}} \boldsymbol{u}^{(i)} \cdot \boldsymbol{t}_\mathcal{E} ds = \int_{\mathcal{E}^{ij}} \boldsymbol{u}^{(j)} \cdot \boldsymbol{t}_\mathcal{E} ds.$$

We make a change of variables in order to work explicitly with these primal variables, similar to what is done in [23, Section 3.3]. The complementary dual space will then be represented by elements with zero values at the primal degrees of freedom, i.e., they will satisfy

$$\int_\mathcal{E} \boldsymbol{u}^{(i)}_\Delta \cdot \boldsymbol{t}_\mathcal{E} ds = 0$$

for all the subdomain edges $\mathcal{E} \in S_{\mathcal{E}_i}$.

We will also use the following product spaces, which allow discontinuities across the interface:

$$W_0 := \prod_{i=1}^N W^{(i)}, \; W_I := \prod_{i=1}^N W^{(i)}_I, \; W_\Gamma := \prod_{i=1}^N W^{(i)}_\Gamma,$$

and

$$W_\Delta := \prod_{i=1}^N W^{(i)}_\Delta, \; W_\Pi := \prod_{i=1}^N W^{(i)}_\Pi.$$

We then have

$$W_0 = W_I \oplus W_\Gamma = W_I \oplus W_\Delta \oplus W_\Pi.$$

The finite element solutions have a continuous tangential component across the interface and we denote the corresponding subspace of W_Γ by $\widehat{W}_\Gamma$; generally, functions in W_Γ do not satisfy this condition. We also introduce a subspace $\widetilde{W}_\Gamma$, intermediate between $\widehat{W}_\Gamma$ and W_Γ, for which all the primal constraints are enforced. We can then decompose

$$\widehat{W}_\Gamma := \widehat{W}_\Delta \oplus \widehat{W}_\Pi, \;\; \widetilde{W}_\Gamma := W_\Delta \oplus \widehat{W}_\Pi,$$

where $\widehat{W}_\Delta$ is the continuous dual variable subspace and $\widehat{W}_\Pi$ is the continuous primal variable subspace.

The restriction of our problem to the subdomain Ω_i can be written in terms of the local stiffness matrix $A^{(i)}$ and the local right hand side $\boldsymbol{f}^{(i)}$,

$$A^{(i)} = \begin{pmatrix} A_{II}^{(i)} & A_{I\Delta}^{(i)} & A_{I\Pi}^{(i)} \\ A_{\Delta I}^{(i)} & A_{\Delta\Delta}^{(i)} & A_{\Delta\Pi}^{(i)} \\ A_{\Pi I}^{(i)} & A_{\Pi\Delta}^{(i)} & A_{\Pi\Pi}^{(i)} \end{pmatrix}, \; \boldsymbol{f}^{(i)} = \begin{pmatrix} \boldsymbol{f}_I^{(i)} \\ \boldsymbol{f}_\Delta^{(i)} \\ \boldsymbol{f}_\Pi^{(i)} \end{pmatrix}. \tag{2.3}$$

We can express the global linear system by assembling the local subdomain problems as

$$A \begin{pmatrix} \boldsymbol{u}_I \\ \boldsymbol{u}_\Delta \\ \boldsymbol{u}_\Pi \end{pmatrix} = \begin{pmatrix} A_{II} & A_{I\Delta} & A_{I\Pi} \\ A_{\Delta I} & A_{\Delta\Delta} & A_{\Delta\Pi} \\ A_{\Pi I} & A_{\Pi\Delta} & A_{\Pi\Pi} \end{pmatrix} \begin{pmatrix} \boldsymbol{u}_I \\ \boldsymbol{u}_\Delta \\ \boldsymbol{u}_\Pi \end{pmatrix} = \begin{pmatrix} \boldsymbol{f}_I \\ \boldsymbol{f}_\Delta \\ \boldsymbol{f}_\Pi \end{pmatrix}, \tag{2.4}$$

with $\boldsymbol{u}_I \in W_I$, $\boldsymbol{u}_\Delta \in \widehat{W}_\Delta$, $\boldsymbol{u}_\Pi \in \widehat{W}_\Pi$.

3. The BDDC methods. In this section, we describe our BDDC algorithm. We start by defining some operators that we will also use in our analysis. We first consider restriction operators. Let

$$\widehat{R}_\Gamma^{(i)} : \widehat{W}_\Gamma \to W_\Gamma^{(i)}, \widetilde{R}_\Gamma^{(i)} : \widetilde{W}_\Gamma \to W_\Gamma^{(i)}$$

be the operators that map global interface vectors defined on Γ to their components on Γ_i. Similarly, we define

$$R_\Delta^{(i)} : W_\Delta \to W_\Delta^{(i)}, R_\Pi^{(i)} : \widehat{W}_\Pi \to W_\Pi^{(i)}, \widetilde{R}_{\Gamma\Delta} : \widetilde{W}_\Gamma \to W_\Delta,$$

$$\widetilde{R}_{\Gamma\Pi} : \widetilde{W}_\Gamma \to \widehat{W}_\Pi \text{ and } R_{\Gamma\Delta}^{(i)} : W_\Gamma^{(i)} \to W_\Delta^{(i)}.$$

We consider the direct sums $\widehat{R}_\Gamma := \bigoplus_{i=1}^{N} \widehat{R}_\Gamma^{(i)}$ and $\overline{R}_\Gamma := \bigoplus_{i=1}^{N} \widetilde{R}_\Gamma^{(i)}$. Furthermore, $\widetilde{R}_\Gamma : \widehat{W}_\Gamma \to \widetilde{W}_\Gamma$ will be the direct sum of $\widehat{R}_\Pi$ and the $\widehat{R}_\Delta^{(i)}$, where $\widehat{R}_\Pi : \widehat{W}_\Gamma \to \widehat{W}_\Pi$ and $\widehat{R}_\Delta^{(i)} : \widehat{W}_\Gamma \to W_\Delta^{(i)}$ are the corresponding restriction operators.

We next introduce scaling matrices $D^{(i)}$, acting on the degrees of freedom associated with Γ_i. They are combined into a block diagonal matrix and should provide a discrete partition of unity, i.e.,

$$\widehat{R}_\Gamma^T \begin{pmatrix} D^{(1)} & & & \\ & D^{(2)} & & \\ & & \ddots & \\ & & & D^{(N)} \end{pmatrix} \widehat{R}_\Gamma = I. \tag{3.1}$$

We then define the scaled operators $R_{D,\Gamma}^{(i)} := D^{(i)} \widehat{R}_\Gamma^{(i)}$, $\widetilde{R}_{D,\Delta}^{(i)} := R_{\Gamma\Delta}^{(i)} R_{D,\Gamma}^{(i)}$. We next consider a globally scaled operator $\widetilde{R}_{D,\Gamma} := \widehat{R}_\Pi \oplus \left(\bigoplus_{i=1}^N \widetilde{R}_{D,\Delta}^{(i)} \right)$. From (3.1), it follows that

$$\widetilde{R}_\Gamma^T \widetilde{R}_{D,\Gamma} = \widetilde{R}_{D,\Gamma}^T \widetilde{R}_\Gamma = I. \tag{3.2}$$

Finally, we introduce an averaging operator $E_D : \widetilde{W}_\Gamma \to \widehat{W}_\Gamma$ by

$$E_D := \widetilde{R}_\Gamma \widetilde{R}_{D,\Gamma}^T. \tag{3.3}$$

This operator is a projection, i.e., $E_D^2 = E_D$; this follows from (3.2) and therefore E_D provides a weighted average across the interface Γ.

We will consider the subdomain Schur complements

$$S_\Gamma^{(i)} := A_{\Gamma\Gamma}^{(i)} - A_{\Gamma I}^{(i)} {A_{II}^{(i)}}^{-1} A_{I\Gamma}^{(i)}, \tag{3.4}$$

where

$$A_{\Gamma\Gamma}^{(i)} := \begin{pmatrix} A_{\Delta\Delta}^{(i)} & A_{\Delta\Pi}^{(i)} \\ A_{\Pi\Delta}^{(i)} & A_{\Pi\Pi}^{(i)} \end{pmatrix}$$

is the block matrix corresponding to the interface degrees of freedom in (2.3). From (3.4), we note that we can compute $S_\Gamma^{(i)}$ times a vector by a local computation involving Ω_i; the application of the inverse of $A_{II}^{(i)}$ to a vector corresponds to the solution of a Dirichlet problem in Ω_i. Similarly, we can find ${S_\Gamma^{(i)}}^{-1} \boldsymbol{u}_\Gamma^{(i)}$ by solving a linear system with the matrix $A^{(i)}$ and right hand side $(\boldsymbol{0}, \boldsymbol{u}_\Gamma^{(i)})^T$. Hence, we do not need to compute the elements of the Schur complements.

We denote the global Schur complement by S_Γ, given by the direct sum of the local Schur complements $S_\Gamma^{(i)}$. By using the local Schur complements, we can build a global interface problem. By eliminating the interior variables, the global problem (2.4) can thus be reduced to

$$\widehat{S}_\Gamma \boldsymbol{u}_\Gamma = \boldsymbol{g}_\Gamma, \tag{3.5}$$

with

$$\widehat{S}_\Gamma := \sum_{i=1}^N {\widehat{R}_\Gamma^{(i)}}^T S_\Gamma^{(i)} \widehat{R}_\Gamma^{(i)} = \widehat{R}_\Gamma^T S_\Gamma \widehat{R}_\Gamma,$$

and

$$\boldsymbol{g}_\Gamma := \sum_{i=1}^N {\widehat{R}_\Gamma^{(i)}}^T \left[\begin{pmatrix} \boldsymbol{f}_\Delta^{(i)} \\ \boldsymbol{f}_\Pi^{(i)} \end{pmatrix} - \begin{pmatrix} A_{\Delta I}^{(i)} \\ A_{\Pi I}^{(i)} \end{pmatrix} {A_{II}^{(i)}}^{-1} \boldsymbol{f}_I^{(i)} \right].$$

We will build a preconditioner for (3.5). Once $\boldsymbol{u}_\Gamma^{(i)}$ has been found, $\boldsymbol{u}_I^{(i)}$ is found by solving

$$A_{II}^{(i)} \boldsymbol{u}_I^{(i)} = \boldsymbol{f}_I^{(i)} - \left(A_{I\Delta}^{(i)} A_{I\Pi}^{(i)} \right) \boldsymbol{u}_\Gamma^{(i)}.$$

We now consider a Schur complement $\widetilde{S}_\Gamma$ on the space $\widetilde{W}_\Gamma$: given $\boldsymbol{u}_\Gamma \in \widetilde{W}_\Gamma$, $\widetilde{S}_\Gamma \boldsymbol{u}_\Gamma \in \widetilde{W}_\Gamma$ is determined such that

$$\begin{pmatrix} A_{II}^{(1)} & {A_{\Delta I}^{(1)}}^T & & & & {\widehat{A}_{\Pi I}^{(1)}}^T \\ A_{\Delta I}^{(1)} & A_{\Delta\Delta}^{(1)} & & & & {\widehat{A}_{\Pi\Delta}^{(1)}}^T \\ & & \ddots & & & \vdots \\ & & & A_{II}^{(N)} & {A_{\Delta I}^{(N)}}^T & {\widehat{A}_{\Pi I}^{(N)}}^T \\ & & & A_{\Delta I}^{(N)} & A_{\Delta\Delta}^{(N)} & {\widehat{A}_{\Pi\Delta}^{(N)}}^T \\ \widehat{A}_{\Pi I}^{(1)} & \widehat{A}_{\Pi\Delta}^{(1)} & \cdots & \widehat{A}_{\Pi I}^{(N)} & \widehat{A}_{\Pi\Delta}^{(N)} & \widehat{A}_{\Pi\Pi} \end{pmatrix} \begin{pmatrix} \boldsymbol{u}_I^{(1)} \\ \boldsymbol{u}_\Delta^{(1)} \\ \vdots \\ \boldsymbol{u}_I^{(N)} \\ \boldsymbol{u}_\Delta^{(N)} \\ \boldsymbol{u}_\Pi \end{pmatrix} = \begin{pmatrix} 0 \\ R_\Delta^{(1)} \widetilde{R}_{\Gamma\Delta} \widetilde{S}_\Gamma \boldsymbol{u}_\Gamma \\ \vdots \\ 0 \\ R_\Delta^{(N)} \widetilde{R}_{\Gamma\Delta} \widetilde{S}_\Gamma \boldsymbol{u}_\Gamma \\ \widetilde{R}_{\Gamma\Pi} \widetilde{S}_\Gamma \boldsymbol{u}_\Gamma \end{pmatrix}.$$

Here,

$$\widehat{A}_{\Pi I}^{(i)} = {R_\Pi^{(i)}}^T A_{\Pi I}^{(i)}, \ \widehat{A}_{\Pi\Delta}^{(i)} = {R_\Pi^{(i)}}^T A_{\Pi\Delta}^{(i)}, \ \forall i = 1, \ldots, N,$$

and

$$\widehat{A}_{\Pi\Pi} = \sum_{i=1}^N {R_\Pi^{(i)}}^T A_{\Pi\Pi}^{(i)} R_\Pi^{(i)}.$$

We note that $\widetilde{S}_\Gamma = \overline{R}_\Gamma^T S_\Gamma \overline{R}_\Gamma$, and by using restriction and extension operators, we also find that $\widehat{S}_\Gamma = \widetilde{R}_\Gamma^T \widetilde{S}_\Gamma \widetilde{R}_\Gamma$. Then, (3.5) can be rewritten as

$$\widetilde{R}_\Gamma^T \widetilde{S}_\Gamma \widetilde{R}_\Gamma \boldsymbol{u}_\Gamma = \boldsymbol{g}_\Gamma. \tag{3.6}$$

The inverse of $\widetilde{S}_\Gamma$ can be evaluated by Cholesky elimination; see, e.g., [23, 27]. We have

$$\widetilde{S}_\Gamma^{-1} = \widetilde{R}_{\Gamma\Delta}^T \left(\sum_{i=1}^N \left(0 \; {R_\Delta^{(i)}}^T\right) \begin{pmatrix} A_{II}^{(i)} & A_{I\Delta}^{(i)} \\ A_{\Delta I}^{(i)} & A_{\Delta\Delta}^{(i)} \end{pmatrix}^{-1} \begin{pmatrix} 0 \\ R_\Delta^{(i)} \end{pmatrix} \right) \widetilde{R}_{\Gamma\Delta} + \Phi S_{\Pi\Pi}^{-1} \Phi^T,$$

with

$$\Phi := \widetilde{R}_{\Gamma\Pi}^T - \widetilde{R}_{\Gamma\Delta}^T \sum_{i=1}^N \left(0 \; {R_\Delta^{(i)}}^T\right) \begin{pmatrix} A_{II}^{(i)} & A_{I\Delta}^{(i)} \\ A_{\Delta I}^{(i)} & A_{\Delta\Delta}^{(i)} \end{pmatrix}^{-1} \begin{pmatrix} {A_{\Pi I}^{(i)}}^T \\ {A_{\Pi\Delta}^{(i)}}^T \end{pmatrix} R_\Pi^{(i)}$$

and where

$$S_{\Pi\Pi} := \sum_{i=1}^N {R_\Pi^{(i)}}^T \left(A_{\Pi\Pi}^{(i)} - \left(A_{\Pi I}^{(i)} \; A_{\Pi\Delta}^{(i)}\right) \begin{pmatrix} A_{II}^{(i)} & A_{I\Delta}^{(i)} \\ A_{\Delta I}^{(i)} & A_{\Delta\Delta}^{(i)} \end{pmatrix}^{-1} \begin{pmatrix} {A_{\Pi I}^{(i)}}^T \\ {A_{\Pi\Delta}^{(i)}}^T \end{pmatrix} \right) R_\Pi^{(i)}.$$

Finally, we define the weighted operators $D^{(i)}$. For our deluxe scaling, we consider the Schur complements related to a coarse edge $\mathcal{E}^{ij}$. Let

$$A_{\mathcal{E}^{ij}}^{(k)} := \begin{pmatrix} A_{II}^{(k)} & A_{I\mathcal{E}^{ij}}^{(k)} \\ A_{\mathcal{E}^{ij}I}^{(k)} & A_{\mathcal{E}^{ij}\mathcal{E}^{ij}}^{(k)} \end{pmatrix},$$

for $k \in \{i, j\}$. The two Schur complements associated with $\mathcal{E}^{ij}$ are given by

$$S_{\mathcal{E}^{ij}}^{(k)} := A_{\mathcal{E}^{ij}\mathcal{E}^{ij}}^{(k)} - A_{\mathcal{E}^{ij}I}^{(k)} {A_{II}^{(k)}}^{-1} A_{I\mathcal{E}^{ij}}^{(k)} \tag{3.7}$$

for $k \in \{i, j\}$. We define the scaling matrices $D_j^{(i)} := \left(S_{\mathcal{E}^{ij}}^{(i)} + S_{\mathcal{E}^{ij}}^{(j)}\right)^{-1} S_{\mathcal{E}^{ij}}^{(i)}$. The scaling deluxe operator $D^{(i)}$ is given by

$$D^{(i)} := \begin{pmatrix} D_{j_1}^{(i)} & & & \\ & D_{j_2}^{(i)} & & \\ & & \ddots & \\ & & & D_{j_k}^{(i)} \end{pmatrix}$$

where $j_1, \ldots, j_k \in \Xi_i$, with Ξ_i the set of indices of the subdomains Ω_j, $j \neq i$, which share a subdomain edge with Ω_i. Denote by $\boldsymbol{u}_{\mathcal{E}^{ij}}^{(i)} := R_{\mathcal{E}^{ij}} \boldsymbol{u}^{(i)}$ the restriction to the edge $\mathcal{E}^{ij}$. We can rewrite the average over $\mathcal{E}^{ij}$ as

$$\overline{\boldsymbol{u}}_{\mathcal{E}^{ij}} = \left(S_{\mathcal{E}^{ij}}^{(i)} + S_{\mathcal{E}^{ij}}^{(j)}\right)^{-1} \left(S_{\mathcal{E}^{ij}}^{(i)} \boldsymbol{u}_{\mathcal{E}^{ij}}^{(i)} + S_{\mathcal{E}^{ij}}^{(j)} \boldsymbol{u}_{\mathcal{E}^{ij}}^{(j)}\right).$$

With these operators, we define the deluxe BDDC preconditioner as

$$M_{BDDC}^{-1} := \widetilde{R}_{D,\Gamma}^T \widetilde{S}_\Gamma^{-1} \widetilde{R}_{D,\Gamma}, \tag{3.8}$$

and, from (3.6), the preconditioned linear system is given by

$$M_{BDDC}^{-1} \widehat{S}_\Gamma \boldsymbol{u}_\Gamma = \widetilde{R}_{D,\Gamma}^T \widetilde{S}_\Gamma^{-1} \widetilde{R}_{D,\Gamma} \widetilde{R}_\Gamma^T \widetilde{S}_\Gamma \widetilde{R}_\Gamma \boldsymbol{u}_\Gamma = \widetilde{R}_{D,\Gamma}^T \widetilde{S}_\Gamma^{-1} \widetilde{R}_{D,\Gamma} \boldsymbol{g}_\Gamma. \tag{3.9}$$

We next define norms related to the Schur complements. The S_Γ-norm is given by $\|\boldsymbol{u}_\Gamma\|_{S_\Gamma}^2 := \boldsymbol{u}_\Gamma^T S_\Gamma \boldsymbol{u}_\Gamma$ for $\boldsymbol{u}_\Gamma \in W_\Gamma$. Similar expressions can be written for $\|\boldsymbol{u}_\Gamma^{(i)}\|_{S_\Gamma^{(i)}}^2$, $\|\boldsymbol{u}_\mathcal{E}^{(i)}\|_{S_\mathcal{E}^{(i)}}^2$ and $\|\tilde{\boldsymbol{u}}_\Gamma\|_{\widetilde{S}_\Gamma}^2$. It is easy to see that $\|\tilde{\boldsymbol{u}}_\Gamma\|_{\widetilde{S}_\Gamma}^2 = \|\overline{R}_\Gamma \tilde{\boldsymbol{u}}_\Gamma\|_{S_\Gamma}^2$.

The condition number of the BDDC algorithm satisfies (see, e.g., [22, 5]):

$$\kappa(M_{BDDC}^{-1}\widehat{S}_\Gamma) \le \|E_D\|_{\widetilde{S}_\Gamma}^2.$$

Following [5, Theorem 4.4], in order to get an estimate for $\|E_D\|_{\widetilde{S}_\Gamma}^2$, we can reduce the problem to obtaining a bound for $\|R_{\mathcal{E}}^T(\boldsymbol{u}_{\mathcal{E}}^{(i)} - \overline{\boldsymbol{u}}_{\mathcal{E}})\|_{S_\Gamma^{(i)}}$. After some algebra (see Theorem 6.2), it is possible to show that

$$\|R_{\mathcal{E}}^T(\boldsymbol{u}_{\mathcal{E}}^{(i)} - \bar{\boldsymbol{u}}_{\mathcal{E}})\|_{S_\Gamma^{(i)}}^2 + \|R_{\mathcal{E}}^T(\boldsymbol{u}_{\mathcal{E}}^{(j)} - \bar{\boldsymbol{u}}_{\mathcal{E}})\|_{S_\Gamma^{(j)}}^2 \le 2\|\boldsymbol{u}_{\mathcal{E}}^{(i)} - \boldsymbol{u}_{\Pi\mathcal{E}}^{(i)}\|_{S_{\mathcal{E}}^{(i)}}^2 + 2\|\boldsymbol{u}_{\mathcal{E}}^{(j)} - \boldsymbol{u}_{\Pi\mathcal{E}}^{(j)}\|_{S_{\mathcal{E}}^{(j)}}^2, \quad (3.10)$$

where $\boldsymbol{u}_{\Pi\mathcal{E}}^{(i)}$ is the primal component of $\boldsymbol{u}_{\Pi}^{(i)}$ restricted to the edge $\mathcal{E}$. Thus, we only need to obtain local bounds for the individual terms in the right-hand side. For this purpose, we will construct explicit functions with the required tangential data on $\mathcal{E}$ and a proper bound. This construction is presented in Section 5.5, where we closely follow [11, Section 4].

4. Uniform domains. We now introduce some important results about uniform domains.

DEFINITION 4.1 (uniform domain). *A bounded domain $\Omega \in \mathbb{R}^2$ is uniform if there exists a constant $C_U(\Omega) > 0$ such that for any pair of points $\boldsymbol{a}$, $\boldsymbol{b}$ in the closure of Ω, there is a curve $\gamma(t) : [0, l] \to \Omega$, parametrized by arc length, with $\gamma(0) = \boldsymbol{a}$, $\gamma(l) = \boldsymbol{b}$ and with*

$$l \le C_U|\boldsymbol{a} - \boldsymbol{b}|,$$
$$\min(|\gamma(t) - \boldsymbol{a}|, |\gamma(t) - \boldsymbol{b}|) \le C_U\, dist(\gamma(t), \partial\Omega).$$

REMARK 4.2. *For a rectangular domain, $C_U \ge L_1/L_2$, where L_1, L_2 are the height and width of the domain. Thus, the constant C_U can be large if the subdomain has a large aspect ratio.*

Related to the curve γ, we define the following region:

DEFINITION 4.3. *Let $\boldsymbol{a}$ and $\boldsymbol{b}$ denote the endpoints of $\mathcal{E} = \mathcal{E}^{ij} \in S_{\mathcal{E}_i}$. The region $\mathcal{R}_{\mathcal{E}}$ is defined as the open set with boundary $\partial\mathcal{R}_{\mathcal{E}} = \gamma_{\boldsymbol{ab}} \cup \mathcal{E}$, where $\gamma_{\boldsymbol{ab}}$ is the curve γ in Definition 4.1.*

This region $\mathcal{R}_{\mathcal{E}}$ satisfies the following lemma; see [11, Lemma 3.4].

LEMMA 4.4. *Given a uniform subdomain Ω_i and a connected subset $\mathcal{E} \subset \partial\Omega_i$, the region $\mathcal{R}_{\mathcal{E}}$ satisfies*

$$|\mathcal{R}_{\mathcal{E}}| \le (C_U^2/\pi)d_{\mathcal{E}}^2,$$
$$diam(\mathcal{R}_{\mathcal{E}}) \le (2C_U - 1)d_{\mathcal{E}}.$$

We next introduce a modified region $\widehat{\mathcal{R}}_{\mathcal{E}}$ related to $\mathcal{R}_{\mathcal{E}}$:

LEMMA 4.5. *Given a uniform domain Ω_i and a connected subset $\mathcal{E} \subset \partial\Omega_i$, there exist a constant C, depending on $C_U(\Omega_i)$, and a uniform domain $\widehat{\mathcal{R}}_{\mathcal{E}}$, which is a union of finite elements of Ω_i, such that $\mathcal{R}_{\mathcal{E}} \subset \widehat{\mathcal{R}}_{\mathcal{E}}$, $\partial\widehat{\mathcal{R}}_{\mathcal{E}} \cap \partial\Omega_i = \mathcal{E}$, and*

$$|\widehat{\mathcal{R}}_{\mathcal{E}}| \le C d_{\mathcal{E}}^2,$$
$$diam(\widehat{\mathcal{R}}_{\mathcal{E}}) \le C d_{\mathcal{E}}.$$

Proof. See [11, Lemma 3.5]. ☐

We have the following result; see [24, 14].

LEMMA 4.6 (Isoperimetric inequality). *Let $\Omega \subset \mathbb{R}^n$ be a domain — an open, bounded, and connected set — and let u be sufficiently smooth. Then,*

$$\inf_{c\in\mathbb{R}} \left(\int_\Omega |u - c|^{n/(n-1)} dx \right)^{(n-1)/n} \le \gamma(\Omega, n) \int_\Omega |\nabla u| dx, \quad (4.1)$$

if and only if,

$$(\min(|A|,|B|))^{1-1/n} \leq \gamma(\Omega,n)|\partial A \cap \partial B|.$$

Here, $A \subset \Omega$ is an arbitrary open set, and $B = \Omega \setminus \overline{A}$; $\gamma(\Omega,n)$ is the best possible constant and $|A|$ is the measure of the set A, etc.

The parameter $\gamma(\Omega,2)$ is bounded for uniform domains; see [3, 24]. For two dimensions, we immediately obtain a standard Poincaré inequality from (4.1) by using the Cauchy-Schwarz inequality. We note that the best choice of c is $\overline{u}_\Omega$, the average of u over the domain.

LEMMA 4.7 (Poincaré's inequality). *Consider a uniform domain $\Omega \in \mathbb{R}^2$. Then*

$$\|u - \bar{u}_\Omega\|^2_{L^2(\Omega)} \leq (\gamma(\Omega,2))^2|\Omega|\|\nabla u\|^2_{L^2(\Omega)} \ \forall u \in H(grad,\Omega).$$

Finally, we need the following discrete Sobolev inequality, proved in [7, Lemma 3.2] for John domains (and thus in particular for uniform domains, see [17]).

LEMMA 4.8. *For $u \in W^h_{grad}(\Omega)$, there exists a constant C such that*

$$\|u\|^2_{L^\infty(\Omega)} \leq C\left(1 + \log\frac{H}{h}\right)\|u\|^2_{H^1(\Omega)},$$

$$\|u - \bar{u}_\Omega\|^2_{L^\infty(\Omega)} \leq C\left(1 + \log\frac{H}{h}\right)|u|^2_{H^1(\Omega)},$$

where

$$\|u\|^2_{H^1(\Omega)} := |u|^2_{H^1(\Omega)} + \frac{1}{H^2}\|u\|^2_{L^2(\Omega)}$$

and $diam(\Omega) = H$. The constant C depends on the uniform constant $C_U(\Omega)$, the Poincaré parameter $\gamma(\Omega,2)$ and the shape regularity of the elements.

5. Technical Tools.

In this section, we collect some technical tools and define functions that will be used in the proof of our main theorem.

5.1. A Helmholtz decomposition.

The following lemma will allow us to obtain a stable decomposition for functions in $W^h_{\mathrm{curl}}(\Omega_i)$:

LEMMA 5.1. *Given an uniform domain D of diameter d and $\boldsymbol{u} \in W^{h_i}_{curl}(D)$, there exist $p \in W^{h_i}_{grad}(D)$, $\boldsymbol{r} \in W^{h_i}_{curl}(D)$ and a constant C such that*

$$\boldsymbol{u} = \nabla p + \boldsymbol{r},$$

$$\|\nabla p\|^2_{L^2(D)} \leq C\left(\|\boldsymbol{u}\|^2_{L^2(D)} + d^2\|\nabla \times \boldsymbol{u}\|^2_{L^2(D)}\right) \ \text{and} \tag{5.1a}$$

$$\|\boldsymbol{r}\|^2_{L^\infty(D)} \leq C\left(1 + \log\frac{d}{h_i}\right)\|\nabla \times \boldsymbol{u}\|^2_{L^2(D)}. \tag{5.1b}$$

The constant C depends on D and the shape regularity of the mesh.

Proof. See [11, Lemma 3.14]. ☐

5.2. Discrete harmonic extensions.

The space of discrete harmonic functions is directly related to the Schur complements. A function $\boldsymbol{u}^{(i)}$ is said to be discrete harmonic on Ω_i if

$$A^{(i)}_{II}\boldsymbol{u}^{(i)}_I + A^{(i)}_{I\Gamma}\boldsymbol{u}^{(i)}_\Gamma = 0. \tag{5.2}$$

Given $\boldsymbol{u}^{(i)}_\Gamma \in W^{(i)}_\Gamma$, we define the harmonic extension of $\boldsymbol{u}^{(i)}_\Gamma \cdot \boldsymbol{t}_e$ as $\mathcal{H}_i(\boldsymbol{u}^{(i)}_\Gamma \cdot \boldsymbol{t}_e) := \boldsymbol{u}^{(i)}$ where $\boldsymbol{u}^{(i)}$ satisfies (5.2). Clearly $\mathcal{H}_i(\boldsymbol{u}^{(i)}_\Gamma \cdot \boldsymbol{t}_e)$ is completely defined by the tangential data on Γ_i. We have the following lemma:

LEMMA 5.2. *The discrete harmonic extension $\boldsymbol{u}^{(i)} = \mathcal{H}_i(\boldsymbol{u}^{(i)}_\Gamma \cdot \boldsymbol{t}_e)$ of $\boldsymbol{u}^{(i)}_\Gamma \cdot \boldsymbol{t}_e$ into Ω_i satisfies*

$$a_i(\boldsymbol{u}^{(i)},\boldsymbol{u}^{(i)}) = \min_{\boldsymbol{v}^{(i)}\cdot\boldsymbol{t}_e = \boldsymbol{u}^{(i)}_\Gamma\cdot\boldsymbol{t}_e} a_i(\boldsymbol{v}^{(i)},\boldsymbol{v}^{(i)})$$

and

$$\|\boldsymbol{u}_\Gamma^{(i)}\|^2_{S_\Gamma^{(i)}} = a_i(\boldsymbol{u}^{(i)}, \boldsymbol{u}^{(i)}).$$

Proof. See [34, Lemma 4.9]. □

5.3. An inverse inequality. We present an inverse inequality for elements in the space $W^{h_i}_{\mathrm{curl}}(\Omega_i)$ which will be used in our discussion. First, we have the following elementary estimates for a function in $W^{h_i}_{\mathrm{curl}}(\Omega_i)$ in terms of its degrees of freedom defined in (2.1):

LEMMA 5.3. *Let $K \in \mathcal{T}_{h_i}$. Then, there exist strictly positive constants c and C, which depend only on the aspect ratio of K, such that for all $\boldsymbol{u} \in W^{h_i}_{curl}(\Omega_i)$,*

$$c \sum_{e\in\partial K} h_e^2 \lambda_e(\boldsymbol{u})^2 \le \|\boldsymbol{u}\|^2_{L^2(K)} \le C \sum_{e\in\partial K} h_e^2 \lambda_e(\boldsymbol{u})^2,$$

$$\|\nabla \times \boldsymbol{u}\|^2_{L^2(K)} \le C \sum_{e\in\partial K} \lambda_e(\boldsymbol{u})^2.$$

Proof. See [29, Proposition 6.3.1] and [36, Lemma 3.1]. □

Combining these two inequalities, we find an inverse inequality:

COROLLARY 5.4 (Inverse inequality). *For $\boldsymbol{u} \in W^{h_i}_{curl}(\Omega_i)$, there exists a constant C, which depends only on the aspect ratio of K, such that*

$$\|\nabla \times \boldsymbol{u}\|^2_{L^2(K)} \le C h_i^{-2} \|\boldsymbol{u}\|^2_{L^2(K)}. \tag{5.3}$$

5.4. Estimates for auxiliary functions. We borrow some results from [11]. We start by introducing a coarse linear interpolant for functions in $W^{h_i}_{\mathrm{grad}}(\Omega_i)$.

DEFINITION 5.5 (linear interpolant). *Given $f \in W^{h_i}_{grad}(\Omega_i)$ and a subdomain edge $\mathcal{E} \in S_{\mathcal{E}_i}$, we define the linear function*

$$f^{\mathcal{E}\ell}(\boldsymbol{x}) := f(\boldsymbol{a}) + \frac{f(\boldsymbol{b}) - f(\boldsymbol{a})}{d_{\mathcal{E}}}\,(\boldsymbol{x} - \boldsymbol{a}) \cdot \boldsymbol{d}_{\mathcal{E}}.$$

We note that $f^{\mathcal{E}\ell}(\boldsymbol{a}) = f(\boldsymbol{a})$, $f^{\mathcal{E}\ell}(\boldsymbol{b}) = f(\boldsymbol{b})$ and that $f^{\mathcal{E}\ell}$ varies linearly in the direction $\boldsymbol{d}_{\mathcal{E}}$. We will use the following lemmas:

LEMMA 5.6. *Let $\widehat{\mathcal{R}}_{\mathcal{E}}$ be the uniform domain of Lemma 4.5. For any $p \in W^{h_i}_{grad}(\Omega_i)$, there exists a function $p^{\mathcal{E}\Delta} \in W^{h_i}_{grad}(\Omega_i)$ such that $p^{\mathcal{E}\Delta} = p - p^{\mathcal{E}\ell}$ along $\mathcal{E}$. This function vanishes along $\partial\widehat{\mathcal{R}}_{\mathcal{E}} \setminus \mathcal{E}$ and $\partial\Omega_i \setminus \mathcal{E}$, and satisfies*

$$\|\nabla p^{\mathcal{E}\Delta}\|^2_{L^2(\Omega_i)} \le C \left(1 + \log \frac{d_{\mathcal{E}}}{h_i}\right)^2 \|\nabla p\|^2_{L^2(\widehat{\mathcal{R}}_{\mathcal{E}})},$$

for some constant C depending on C_U, $\gamma(\Omega, 2)$ and the shape regularity of the elements.

Proof. See [11, Lemma 3.8]. □

LEMMA 5.7. *Given $\boldsymbol{r} \in W^{h_i}_{curl}(\Omega_i)$ and a subdomain edge $\mathcal{E} \in S_{\mathcal{E}_i}$, it holds that*

$$|\bar{r}_{\mathcal{E}}|^2 \le C \left(\|\boldsymbol{r}\|^2_{L^\infty(\widehat{\mathcal{R}}_{\mathcal{E}})} + \|\nabla \times \boldsymbol{r}\|^2_{L^2(\widehat{\mathcal{R}}_{\mathcal{E}})}\right),$$

where

$$\bar{r}_{\mathcal{E}} := \frac{1}{d_{\mathcal{E}}} \int_{\mathcal{E}} \boldsymbol{r} \cdot \boldsymbol{t}_{\mathcal{E}}\, ds, \tag{5.4}$$

and the constant C depends only on the uniform parameter $C_U(\Omega_i)$.

Proof. This result follows from [11, Lemma 3.10] and the fact that $\mathcal{R}_{\mathcal{E}} \subset \widehat{\mathcal{R}}_{\mathcal{E}}$. □

LEMMA 5.8. *Given* $\boldsymbol{r} \in W^{h_i}_{curl}(\Omega_i)$ *and* $\mathcal{E} \in S_{\mathcal{E}_i}$*, there exists a function* $\boldsymbol{r}^{\mathcal{E}} \in W^{h_i}_{curl}(\Omega_i)$ *such that* $\boldsymbol{r}^{\mathcal{E}} \cdot \boldsymbol{t}_e = \boldsymbol{r} \cdot \boldsymbol{t}_e$ *along* $\mathcal{E}$ *and with vanishing tangential data along* $\partial\widehat{\mathcal{R}}_{\mathcal{E}} \setminus \mathcal{E}$ *and* $\partial\Omega_i \setminus \mathcal{E}$*. Further,*

$$\|\boldsymbol{r}^{\mathcal{E}}\|_{L^2(\Omega_i)} \leq C d_{\mathcal{E}}^2 \|\boldsymbol{r}\|^2_{L^\infty(\widehat{\mathcal{R}}_{\mathcal{E}})},$$

$$\|\nabla \times \boldsymbol{r}^{\mathcal{E}}\|_{L^2(\Omega_i)} \leq C \left(\|\nabla \times \boldsymbol{r}\|_{L^2(\widehat{\mathcal{R}}_{\mathcal{E}})} + \left(1 + \log \frac{d_{\mathcal{E}}}{h_i}\right) \|\boldsymbol{r}\|^2_{L^\infty(\widehat{\mathcal{R}}_{\mathcal{E}})} \right),$$

for some constant C *depending on* C_U *and the shape regularity of the elements.*

Proof. See [11, Lemma 3.12]. ∎

LEMMA 5.9. *Given* $\mathcal{E} \in S_{\mathcal{E}_i}$*, there exists a coarse space function* $\boldsymbol{N}_{\mathcal{E}} \in W^{h_i}_{curl}(\Omega_i)$ *with* $\boldsymbol{N}_{\mathcal{E}} \cdot \boldsymbol{t}_e = \boldsymbol{d}_{\mathcal{E}} \cdot \boldsymbol{t}_e$ *along* $\mathcal{E}$ *and with* $\boldsymbol{N}_{\mathcal{E}} \cdot \boldsymbol{t}_e = 0$ *everywhere else on* $\partial\Omega_i$ *such that*

$$\|\boldsymbol{N}_{\mathcal{E}}\|^2_{L^2(\Omega_i)} \leq C d_{\mathcal{E}}^2,$$

$$\|\nabla \times \boldsymbol{N}_{\mathcal{E}}\|^2_{L^2(\Omega_i)} \leq C \left(1 + \log d_{\mathcal{E}}/h_i\right),$$

for some constant C *depending on* C_U *and the shape regularity of the elements.*

Proof. See [11, Lemma 3.11]. ∎

5.5. A stability estimate. In this section, we will derive an edge lemma that will provide a bound for the terms in the right-hand side of (3.10). For that, we split the set of edges $S_{\mathcal{E}_i}$ into two subsets. We define

$$\hat{d}_i := \max\left(h_i, \sqrt{\alpha_i/\beta_i}\right)$$

and consider the two cases $d_{\mathcal{E}} < \hat{d}_i$ (curl-dominated) and $d_{\mathcal{E}} \geq \hat{d}_i$ (mass-dominated) separately. Accordingly, we partition the set of subdomain edges of Ω_i as

$$S_{\mathcal{E}_i} = S^c_{\mathcal{E}_i} \cup S^m_{\mathcal{E}_i},$$

where $d_{\mathcal{E}} < \hat{d}_i$ for all the edges in $S^c_{\mathcal{E}_i}$, and $d_{\mathcal{E}} \geq \hat{d}_i$ for those in $S^m_{\mathcal{E}_i}$. We will prove the next lemma, using a similar construction as in [11].

LEMMA 5.10. *For* $\boldsymbol{u}^{(i)} \in W^{(i)}$ *and* $\mathcal{E} \in S_{\mathcal{E}_i}$*, there exist* $\boldsymbol{v}^{(i)}_{\mathcal{E}}, \boldsymbol{v}^{(i)}_{\Pi\mathcal{E}} \in W^{(i)}$ *such that*

$$\begin{cases} \lambda_e(\boldsymbol{v}^{(i)}_{\mathcal{E}}) = \lambda_e(\boldsymbol{u}^{(i)}) & \text{if } e \subset \mathcal{E} \\ \lambda_e(\boldsymbol{v}^{(i)}_{\mathcal{E}}) = 0 & \text{if } e \subset \partial\Omega_i \setminus \mathcal{E}, \end{cases} \tag{5.5}$$

and

$$\begin{cases} \lambda_e(\boldsymbol{v}^{(i)}_{\Pi\mathcal{E}}) = \bar{u}_{\mathcal{E}} \boldsymbol{d}_{\mathcal{E}} \cdot \boldsymbol{t}_e & \text{if } e \subset \mathcal{E} \\ \lambda_e(\boldsymbol{v}^{(i)}_{\Pi\mathcal{E}}) = 0 & \text{if } e \subset \partial\Omega_i \setminus \mathcal{E}, \end{cases} \tag{5.6}$$

where $\bar{u}_{\mathcal{E}}$ *is defined in* (2.2)*. Furthermore,*

$$a_i(\boldsymbol{v}^{(i)}_{\mathcal{E}} - \boldsymbol{v}^{(i)}_{\Pi\mathcal{E}}, \boldsymbol{v}^{(i)}_{\mathcal{E}} - \boldsymbol{v}^{(i)}_{\Pi\mathcal{E}}) \leq C\chi^2 \left(1 + \log \frac{H}{h}\right)^2 a_i(\boldsymbol{u}^{(i)}, \boldsymbol{u}^{(i)}),$$

where $\chi = \max_i \max_{\mathcal{E} \in S^m_{\mathcal{E}_i}} \chi_{\mathcal{E}}(\hat{d}_i)$ *and* C *depends only on* $C_U(\Omega_i)$*,* $\gamma(\Omega_i, 2)$ *and the shape regularity of the elements.*

Proof. First, consider an edge $\mathcal{E} \in S^c_{\mathcal{E}_i}$ and its corresponding region $\widehat{\mathcal{R}}_{\mathcal{E}}$ from Lemma 4.5. We use the Helmholtz decomposition from Lemma 5.1 in this region and write $\boldsymbol{u}^{(i)} = \nabla p + \boldsymbol{r}$. Define the functions $\boldsymbol{w}^{\mathcal{E},c}, \boldsymbol{w}^{\mathcal{E},c}_{\Pi} \in W^{(i)}$ by

$$\boldsymbol{w}^{\mathcal{E},c} := \nabla p^{\mathcal{E}\Delta} + \boldsymbol{r}^{\mathcal{E}} + \frac{p(\boldsymbol{b}) - p(\boldsymbol{a})}{d_{\mathcal{E}}} \boldsymbol{N}_{\mathcal{E}} \text{ and} \tag{5.7}$$

$$\boldsymbol{w}^{\mathcal{E},c}_{\Pi} := \left(\frac{p(\boldsymbol{b}) - p(\boldsymbol{a})}{d_{\mathcal{E}}} + \bar{r}_{\mathcal{E}}\right) \boldsymbol{N}_{\mathcal{E}},$$

where $\nabla p^{\mathcal{E}\Delta}$, $\boldsymbol{r}^{\mathcal{E}}$ and $\boldsymbol{N}_{\mathcal{E}}$ are the functions from Lemmas 5.6, 5.8 and 5.9, and $\bar{r}_{\mathcal{E}}$ is given by (5.4). We find that $\boldsymbol{w}^{\mathcal{E},c} \cdot \boldsymbol{t}_e = \boldsymbol{u}^{(i)} \cdot \boldsymbol{t}_e$ and $\boldsymbol{w}_{\Pi}^{\mathcal{E},c} \cdot \boldsymbol{t}_e = \bar{u}_{\mathcal{E}} \boldsymbol{d}_{\mathcal{E}} \cdot \boldsymbol{t}_e$ along $\mathcal{E}$, and that they vanish on $\partial\Omega_i \setminus \mathcal{E}$. Hence, $\boldsymbol{w}^{\mathcal{E},c}$ and $\boldsymbol{w}_{\Pi}^{\mathcal{E},c}$ satisfy (5.5) and (5.6).

We next find bounds for the energy of the components of $\boldsymbol{w}^{\mathcal{E},c}$ and $\boldsymbol{w}_{\Pi}^{\mathcal{E},c}$. First, from Lemma 5.6, (5.1a) and the fact that $\beta_i d_{\mathcal{E}}^2 \leq \alpha_i$ for $\mathcal{E} \in S_{\mathcal{E}_i}^c$, we obtain

$$E_i(\nabla p^{\mathcal{E}\Delta}) = \beta_i \|\nabla p^{\mathcal{E}\Delta}\|_{L^2(\Omega_i)}^2 \leq C \left(1 + \log \frac{d_{\mathcal{E}}}{h_i}\right)^2 E_{\widehat{\mathcal{R}}_{\mathcal{E}}}(\boldsymbol{u}^{(i)}). \tag{5.8}$$

For the second term of (5.7), from Lemma 5.8 and (5.1b), we get

$$\begin{aligned} E_i(\boldsymbol{r}^{\mathcal{E}}) &= \alpha_i \|\nabla \times \boldsymbol{r}^{\mathcal{E}}\|_{L^2(\Omega_i)}^2 + \beta_i \|\boldsymbol{r}^{\mathcal{E}}\|_{L^2(\Omega_i)}^2 \\ &\leq C \left(1 + \log \frac{d_{\mathcal{E}}}{h_i}\right)^2 E_{\widehat{\mathcal{R}}_{\mathcal{E}}}(\boldsymbol{u}^{(i)}), \end{aligned} \tag{5.9}$$

where we have replaced $\nabla \times \boldsymbol{r}$ by $\nabla \times \boldsymbol{u}^{(i)}$, since $\nabla \times \nabla p = 0$. Next, from Lemmas 5.7 and (5.1b),

$$|\bar{r}_{\mathcal{E}}|^2 \leq C \left(1 + \log \frac{d_{\mathcal{E}}}{h_i}\right) \|\nabla \times \boldsymbol{u}^{(i)}\|_{L^2(\widehat{\mathcal{R}}_{\mathcal{E}})}^2. \tag{5.10}$$

Hence, by Lemma 5.9,

$$\begin{aligned} E_i(\bar{r}_{\mathcal{E}} \boldsymbol{N}_{\mathcal{E}}) &= |\bar{r}_{\mathcal{E}}|^2 \left(\alpha_i \|\nabla \times \boldsymbol{N}_{\mathcal{E}}\|_{L^2(\Omega_i)} + \beta_i \|\boldsymbol{N}_{\mathcal{E}}\|_{L^2(\Omega_i)}^2\right) \\ &\leq C \left(1 + \log \frac{d_{\mathcal{E}}}{h_i}\right)^2 E_{\widehat{\mathcal{R}}_{\mathcal{E}}}(\boldsymbol{u}^{(i)}). \end{aligned} \tag{5.11}$$

From (5.8), (5.9) and (5.11), we conclude that

$$a_i(\boldsymbol{w}^{\mathcal{E},c} - \boldsymbol{w}_{\Pi}^{\mathcal{E},c}, \boldsymbol{w}^{\mathcal{E},c} - \boldsymbol{w}_{\Pi}^{\mathcal{E},c}) \leq C \left(1 + \log \frac{d_{\mathcal{E}}}{h_i}\right)^2 E_{\widehat{\mathcal{R}}_{\mathcal{E}}}(\boldsymbol{u}^{(i)}). \tag{5.12}$$

We next consider an edge $\mathcal{E} \in S_{\mathcal{E}_i}^m$. We divide $\mathcal{E}$ in the following way: starting at $\boldsymbol{a}$ and moving towards $\boldsymbol{b}$, we pick $\boldsymbol{p}_1 := \boldsymbol{a}$ and then $\boldsymbol{p}_2 \in \mathcal{E}$ as the edge node closest to the last point of exit of $\mathcal{E}$ from the circular disk of radius $\hat{d}_i$ centered at $\boldsymbol{p}_1$. Similarly, $\boldsymbol{p}_3 \in \mathcal{E}$ is chosen as the edge node closest to the last point of exit of $\mathcal{E}$ from the circular disk of radius $\hat{d}_i$ centered at $\boldsymbol{p}_2$. This process is repeated until $|\boldsymbol{p}_M - \boldsymbol{b}| < \hat{d}_i$, and we then set $\boldsymbol{p}_{M+1} = \boldsymbol{b}$ and we denote the segment of $\mathcal{E}$ between $\boldsymbol{p}_k$ and $\boldsymbol{p}_{k+1}$ by $\mathcal{E}_k$. We have an M on the order of $\chi_{\mathcal{E}}(\hat{d}_i)(d_{\mathcal{E}}/\hat{d}_i)$. By construction, we have that $\hat{d}_i \leq d_{\mathcal{E}_k} \leq 2\hat{d}_i$.

For each subedge $\mathcal{E}_k$, $k = 1, \ldots, M(\mathcal{E}, \hat{d}_i)$, we consider the region $\widehat{\mathcal{R}}_{\mathcal{E}_k}$ from Lemma 4.5 and the corresponding Helmholtz decomposition $\boldsymbol{u}^{(i)} = \nabla p_k + \boldsymbol{r}_k$. For each term, we define $p^{\mathcal{E}_k\Delta}$, $\boldsymbol{r}^{\mathcal{E}_k}$ and $\boldsymbol{N}_{\mathcal{E}_k}$ similarly as in (5.7), and consider

$$\boldsymbol{w}^{\mathcal{E},m} := \sum_{k=1}^{M(\mathcal{E},\hat{d}_i)} \nabla p^{\mathcal{E}_k\Delta} + \boldsymbol{r}^{\mathcal{E}_k} + \bar{p}_{\mathcal{E}_k} \boldsymbol{N}_{\mathcal{E}_k}, \tag{5.13}$$

$$\boldsymbol{w}_{\Pi}^{\mathcal{E},m} := \bar{u}_{\mathcal{E}} \sum_{k=1}^{M(\mathcal{E},\hat{d}_i)} \boldsymbol{N}_{\mathcal{E}_k}, \text{ where } \bar{p}_{\mathcal{E}_k} := \frac{p(\boldsymbol{b}_k) - p(\boldsymbol{a}_k)}{d_{\mathcal{E}_k}}$$

and $\boldsymbol{a}_k$, $\boldsymbol{b}_k$ are the endpoints of $\mathcal{E}_k$. Now, $(\nabla p^{\mathcal{E}_k\Delta} + \boldsymbol{r}^{\mathcal{E}_k} + \bar{p}_{\mathcal{E}_k} \boldsymbol{N}_{\mathcal{E}_k}) \cdot \boldsymbol{t}_e = \boldsymbol{u}^{(i)} \cdot \boldsymbol{t}_e$ along $\mathcal{E}_k$. It vanishes everywhere else on $\mathcal{E}$ and therefore $\boldsymbol{w}^{\mathcal{E},m} \cdot \boldsymbol{t}_e = \boldsymbol{u}^{(i)} \cdot \boldsymbol{t}_e$ along $\mathcal{E}$ and $\boldsymbol{w}^{\mathcal{E},m} \cdot \boldsymbol{t}_e = 0$ along $\partial\Omega_i \setminus \mathcal{E}$. We also obtain that $\boldsymbol{w}_{\Pi}^{\mathcal{E},m} \cdot \boldsymbol{t}_e = \bar{u}_{\mathcal{E}} \boldsymbol{d}_{\mathcal{E}} \cdot \boldsymbol{t}_e$ along $\mathcal{E}$ and that $\boldsymbol{w}_{\Pi}^{\mathcal{E},m} \cdot \boldsymbol{t}_e = 0$ along $\partial\Omega_i \setminus \mathcal{E}$. Hence, the two functions satisfy (5.5) and (5.6).

By a similar argument as the one that led to (5.8), and using the fact that $d_{\mathcal{E}_k} \leq 2\hat{d}_i$, we obtain

$$E_i(\nabla p^{\mathcal{E}_k\Delta}) \leq C\left(1+\log\frac{\hat{d}_i}{h_i}\right)^2 \beta_i\left(\|\boldsymbol{u}^{(i)}\|^2_{L^2(\widehat{\mathcal{R}}_{\mathcal{E}_k})} + \hat{d}_i^2\|\nabla\times\boldsymbol{u}^{(i)}\|^2_{L^2(\widehat{\mathcal{R}}_{\mathcal{E}_k})}\right).$$

From the definition of $\hat{d}_i$, we observe that if $\hat{d}_i = h_i$, we can use the inverse estimate (5.3) to bound the term $h_i^2\|\nabla\times\boldsymbol{u}^{(i)}\|^2_{L^2(\widehat{\mathcal{R}}_{\mathcal{E}_k})}$ by $\|\boldsymbol{u}^{(i)}\|^2_{L^2(\widehat{\mathcal{R}}_{\mathcal{E}_k})}$ and if $\hat{d}_i = \sqrt{\alpha_i/\beta_i}$ it follows that $\beta_i\hat{d}_i^2 = \alpha_i$. In both cases, we can conclude that

$$E_i(\nabla p^{\mathcal{E}_k\Delta}) \leq C\left(1+\log\frac{\hat{d}_i}{h_i}\right)^2 E_{\widehat{\mathcal{R}}_{\mathcal{E}_k}}(\boldsymbol{u}^{(i)}). \tag{5.14}$$

The bound

$$E_i(\boldsymbol{r}^{\mathcal{E}_k}) \leq C\left(1+\log\frac{\hat{d}_i}{h_i}\right)^2 E_{\widehat{\mathcal{R}}_{\mathcal{E}_k}}(\boldsymbol{u}^{(i)}) \tag{5.15}$$

follows similarly as (5.9) by considering both cases for $\hat{d}_i$ as in (5.14). For the third term of (5.13), we have that

$$|\bar{p}_{\mathcal{E}_k}|^2 \leq \frac{C}{\hat{d}_i^2}\left(1+\log\frac{\hat{d}_i}{h_i}\right)\left(\|\boldsymbol{u}^{(i)}\|^2_{L^2(\widehat{\mathcal{R}}_{\mathcal{E}_k})} + \hat{d}_i^2\|\nabla\times\boldsymbol{u}^{(i)}\|^2_{L^2(\widehat{\mathcal{R}}_{\mathcal{E}_k})}\right), \tag{5.16}$$

where we have used Lemma 4.8 and (5.1a). By Lemma 5.9,

$$E_i(\boldsymbol{N}_{\mathcal{E}_k}) \leq C\beta_i\hat{d}_i^2\left(1+\log\frac{\hat{d}_i}{h_i}\right), \tag{5.17}$$

since $\alpha_i \leq \beta_i\hat{d}_i^2$. From (5.16) and (5.17), we deduce that

$$E_i(\bar{p}_{\mathcal{E}_k}\boldsymbol{N}_{\mathcal{E}_k}) \leq C\left(1+\log\frac{\hat{d}_i}{h_i}\right)^2 \beta_i\left(\|\boldsymbol{u}^{(i)}\|^2_{L^2(\widehat{\mathcal{R}}_{\mathcal{E}_k})} + \hat{d}_i^2\|\nabla\times\boldsymbol{u}^{(i)}\|^2_{L^2(\widehat{\mathcal{R}}_{\mathcal{E}_k})}\right).$$

By considering both cases for $\hat{d}_i$ as in (5.14), we obtain

$$E_i(\bar{p}_{\mathcal{E}_k}\boldsymbol{N}_{\mathcal{E}_k}) \leq C\left(1+\log\frac{\hat{d}_i}{h_i}\right)^2 E_{\widehat{\mathcal{R}}_{\mathcal{E}_k}}(\boldsymbol{u}^{(i)}). \tag{5.18}$$

Now, since $\bar{u}_{\mathcal{E}} = \frac{1}{d_{\mathcal{E}}}\sum_{k=1}^{M(\mathcal{E},\hat{d}_i)}\int_{\mathcal{E}_k}(\nabla p_k + \boldsymbol{r}_k)\cdot\boldsymbol{t}_{\mathcal{E}}\,ds$, by Cauchy-Schwarz and the fact that $M(\mathcal{E},\hat{d}_i)$ is of order $\chi_{\mathcal{E}}(\hat{d}_i)d_{\mathcal{E}}/\hat{d}_i$, we have

$$\begin{aligned}
|\bar{u}_{\mathcal{E}}|^2 &\leq \frac{C}{d_{\mathcal{E}}^2}\chi_{\mathcal{E}}(\hat{d}_i)\frac{d_{\mathcal{E}}}{\hat{d}_i}\sum_{k=1}^{M(\mathcal{E},\hat{d}_i)} d_{\mathcal{E}_k}^2\left(|\bar{p}_{\mathcal{E}_k}|^2 + |\bar{r}_{\mathcal{E}_k}|^2\right)\\
&\leq \frac{C\chi_{\mathcal{E}}(\hat{d}_i)}{d_{\mathcal{E}}\hat{d}_i}\left(1+\log\frac{\hat{d}_i}{h_i}\right)\sum_{k=1}^{M(\mathcal{E},\hat{d}_i)}\left(\|\boldsymbol{u}^{(i)}\|^2_{L^2(\widehat{\mathcal{R}}_{\mathcal{E}_k})} + \hat{d}_i^2\|\nabla\times\boldsymbol{u}^{(i)}\|^2_{L^2(\widehat{\mathcal{R}}_{\mathcal{E}_k})}\right)\\
&\leq \frac{C\chi_{\mathcal{E}}(\hat{d}_i)}{\beta_i d_{\mathcal{E}}\hat{d}_i}\left(1+\log\frac{\hat{d}_i}{h_i}\right)\sum_{k=1}^{M(\mathcal{E},\hat{d}_i)} E_{\widehat{\mathcal{R}}_{\mathcal{E}_k}}(\boldsymbol{u}^{(i)})\\
&\leq \frac{C\chi_{\mathcal{E}}(\hat{d}_i)}{\beta_i d_{\mathcal{E}}\hat{d}_i}\left(1+\log\frac{\hat{d}_i}{h_i}\right) E_{\widetilde{\mathcal{R}}_{\mathcal{E}}}(\boldsymbol{u}^{(i)}),
\end{aligned} \tag{5.19}$$

with $\widetilde{\mathcal{R}}_{\mathcal{E}} = \cup_k \widehat{\mathcal{R}}_{\mathcal{E}_k}$. Here we have used (5.16) and (5.10) in the second step, and the fact that each $\widehat{\mathcal{R}}_{\mathcal{E}_k}$ intersects only a bounded number of other such regions in the last inequality.

From (5.17) and (5.19), we obtain

$$E_i(\boldsymbol{w}_\Pi^{\mathcal{E},m}) \leq C\chi_{\mathcal{E}}^2(\hat{d}_i)\left(1+\log\frac{\hat{d}_i}{h_i}\right)^2 E_{\widetilde{\mathcal{R}}_{\mathcal{E}}}(\boldsymbol{u}^{(i)}). \tag{5.20}$$

Hence, from (5.14), (5.15), (5.18) and (5.20), we obtain

$$a_i(\boldsymbol{w}^{\mathcal{E},m} - \boldsymbol{w}_\Pi^{\mathcal{E},m}, \boldsymbol{w}^{\mathcal{E},m} - \boldsymbol{w}_\Pi^{\mathcal{E},m}) \leq C\chi_{\mathcal{E}}^2(\hat{d}_i)\left(1+\log\frac{\hat{d}_i}{h_i}\right)^2 E_{\widetilde{\mathcal{R}}_{\mathcal{E}}}(\boldsymbol{u}^{(i)}). \tag{5.21}$$

Finally, for $\mathcal{E} \in S_{\mathcal{E}_i}$ consider the functions $\boldsymbol{v}_{\mathcal{E}}^{(i)}, \boldsymbol{v}_{\Pi\mathcal{E}}^{(i)}$ defined by

$$\boldsymbol{v}_{\mathcal{E}}^{(i)} := \begin{cases} \boldsymbol{w}^{\mathcal{E},c} & \text{if } \mathcal{E} \in S_{\mathcal{E}_i}^c \\ \boldsymbol{w}^{\mathcal{E},m} & \text{if } \mathcal{E} \in S_{\mathcal{E}_i}^m \end{cases}, \quad \boldsymbol{v}_{\Pi\mathcal{E}}^{(i)} := \begin{cases} \boldsymbol{w}_\Pi^{\mathcal{E},c} & \text{if } \mathcal{E} \in S_{\mathcal{E}_i}^c \\ \boldsymbol{w}_\Pi^{\mathcal{E},m} & \text{if } \mathcal{E} \in S_{\mathcal{E}_i}^m \end{cases}.$$

By (5.12) and (5.21),

$$a_i(\boldsymbol{v}_{\mathcal{E}}^{(i)} - \boldsymbol{v}_{\Pi\mathcal{E}}^{(i)}, \boldsymbol{v}_{\mathcal{E}}^{(i)} - \boldsymbol{v}_{\Pi\mathcal{E}}^{(i)}) \leq C\chi^2\left(1+\log\frac{H}{h}\right)^2 a_i(\boldsymbol{u}^{(i)}, \boldsymbol{u}^{(i)}).$$

Also, these functions satisfy conditions (5.5) and (5.6) and the lemma holds. ◻

We are now ready to prove the following edge extension lemma:

LEMMA 5.11. *Given $\boldsymbol{u}_\Gamma^{(i)} = \boldsymbol{u}_\Pi^{(i)} + \boldsymbol{u}_\Delta^{(i)} \in W_\Gamma^{(i)}$, denote by $\boldsymbol{u}_{\mathcal{E}}^{(i)}$ and $\boldsymbol{u}_{\Pi\mathcal{E}}^{(i)}$ the restrictions of $\boldsymbol{u}_\Gamma^{(i)}$ and $\boldsymbol{u}_\Pi^{(i)}$ to the subdomain edge $\mathcal{E}$. There exists a constant C, independent of α_i, β_i, h_i and H_i, such that*

$$\|\boldsymbol{u}_{\mathcal{E}}^{(i)} - \boldsymbol{u}_{\Pi\mathcal{E}}^{(i)}\|_{S_{\mathcal{E}}^{(i)}}^2 \leq C\chi^2\left(1+\log\frac{H}{h}\right)^2 \|\boldsymbol{u}_\Gamma^{(i)}\|_{S_\Gamma^{(i)}}^2.$$

Proof. Let $\boldsymbol{u}^{(i)} := \mathcal{H}_i(\boldsymbol{u}_\Gamma^{(i)} \cdot \boldsymbol{t}_e)$ be the harmonic extension of $\boldsymbol{u}_\Gamma^{(i)} \cdot \boldsymbol{t}_e$ over Ω_i. By Lemma 5.10 applied to $\boldsymbol{u}^{(i)}$, there exist $\boldsymbol{v}_{\mathcal{E}}^{(i)}$ and $\boldsymbol{v}_{\Pi\mathcal{E}}^{(i)}$ such that

$$\begin{aligned}
\|\boldsymbol{u}_{\mathcal{E}}^{(i)} - \boldsymbol{u}_{\Pi\mathcal{E}}^{(i)}\|_{S_{\mathcal{E}}^{(i)}}^2 &\leq a_i(\boldsymbol{v}_{\mathcal{E}}^{(i)} - \boldsymbol{v}_{\Pi\mathcal{E}}^{(i)}, \boldsymbol{v}_{\mathcal{E}}^{(i)} - \boldsymbol{v}_{\Pi\mathcal{E}}^{(i)}) \\
&\leq C\chi^2\left(1+\log\frac{H}{h}\right)^2 a_i(\boldsymbol{u}^{(i)}, \boldsymbol{u}^{(i)}) \\
&= C\chi^2\left(1+\log\frac{H}{h}\right)^2 \|\boldsymbol{u}_\Gamma^{(i)}\|_{S_\Gamma^{(i)}}^2,
\end{aligned}$$

where we have used Lemma 5.2 and the fact that $\lambda_e(\boldsymbol{u}_{\mathcal{E}}^{(i)}) = \lambda_e(\boldsymbol{v}_{\mathcal{E}}^{(i)})$ and $\lambda_e(\boldsymbol{u}_{\Pi\mathcal{E}}^{(i)}) = \lambda_e(\boldsymbol{v}_{\Pi\mathcal{E}}^{(i)})$ for $e \subset \partial\Omega_i$. ◻

6. Condition number.

In this section, we present the proof of our main result, Theorem 6.2. The analysis is done in a similar way as in [27, Section 4.2].

LEMMA 6.1. *For $\boldsymbol{u} \in \widehat{W}_\Gamma$, we have that $\boldsymbol{u}^T M_{BDDC} \boldsymbol{u} \leq \boldsymbol{u}^T \widehat{S}_\Gamma \boldsymbol{u}$. In particular, the eigenvalues of the BDDC deluxe operator are bounded from below by 1. Furthermore, if $\|E_D \boldsymbol{u}\|_{\widetilde{S}_\Gamma}^2 \leq C_E \|\boldsymbol{u}\|_{\widetilde{S}_\Gamma}^2$ for all $\boldsymbol{u} \in \widetilde{W}_\Gamma$, then the eigenvalues of the BDDC deluxe operator are bounded from above by C_E.*

Proof. See [22, Theorem 1] ◻

THEOREM 6.2. *The condition number of the BDDC deluxe operator defined in* (3.8) *satisfies*

$$\kappa(M_{BDDC}^{-1}\widehat{S}) \leq C\chi^2|\Xi|\left(1+\log\frac{H}{h}\right)^2,$$

for some constant C that is independent of H, h, β and α. Here $\chi = \max_i \max_{\mathcal{E}\in S^m_{\mathcal{E}_i}} \chi_{\mathcal{E}}(\hat{d}_i)$ and $|\Xi| = \max_i |\Xi_i|$ is the maximum number of subdomain edges for any subdomain.

Proof. We have that

$$\begin{aligned} \|E_D \boldsymbol{u}_\Gamma\|^2_{\widetilde{S}_\Gamma} &\le 2\left(\|\boldsymbol{u}_\Gamma\|^2_{\widetilde{S}_\Gamma} + \|\boldsymbol{u}_\Gamma - E_D\boldsymbol{u}_\Gamma\|^2_{\widetilde{S}_\Gamma}\right) \\ &= 2\left(\|\boldsymbol{u}_\Gamma\|^2_{\widetilde{S}_\Gamma} + \|\overline{R}_\Gamma(\boldsymbol{u}_\Gamma - E_D\boldsymbol{u}_\Gamma)\|^2_{S_\Gamma}\right) \\ &= 2\left(\|\boldsymbol{u}_\Gamma\|^2_{\widetilde{S}_\Gamma} + \sum_{i=1}^N \|\widetilde{R}^{(i)}_\Gamma(\boldsymbol{u}_\Gamma - E_D\boldsymbol{u}_\Gamma)\|^2_{S^{(i)}_\Gamma}\right). \end{aligned}$$

Let $\boldsymbol{u}^{(i)}_\Gamma := \widetilde{R}^{(i)}_\Gamma \boldsymbol{u}_\Gamma$ and denote by $\boldsymbol{u}^{(i)}_{\mathcal{E}}$, $\boldsymbol{u}^{(j)}_{\mathcal{E}}$ the restrictions of $\boldsymbol{u}^{(i)}_\Gamma$ and $\boldsymbol{u}^{(j)}_\Gamma$ to the common edge $\mathcal{E}$. We have that $\widetilde{R}^{(i)}_\Gamma(\boldsymbol{u}_\Gamma - E_D\boldsymbol{u}_\Gamma) = D^{(j)}_i(\boldsymbol{u}^{(i)}_{\mathcal{E}} - \boldsymbol{u}^{(j)}_{\mathcal{E}})$ on $\mathcal{E}$. Hence,

$$\|\widetilde{R}^{(i)}_\Gamma(\boldsymbol{u}_\Gamma - E_D\boldsymbol{u}_\Gamma)\|^2_{S^{(i)}_\Gamma} = \sum_{j\ne i, \mathcal{E}\subset\partial\Omega_i} \|D^{(j)}_i(\boldsymbol{u}^{(i)}_{\mathcal{E}} - \boldsymbol{u}^{(j)}_{\mathcal{E}})\|^2_{S^{(i)}_{\mathcal{E}}}$$

and

$$\|E_D\boldsymbol{u}_\Gamma\|^2_{\widetilde{S}_\Gamma} \le 2\left(\|\boldsymbol{u}_\Gamma\|^2_{\widetilde{S}_\Gamma} + \sum_{\mathcal{E}\in S_{\mathcal{E}}} \|D^{(j)}_i(\boldsymbol{u}^{(i)}_{\mathcal{E}} - \boldsymbol{u}^{(j)}_{\mathcal{E}})\|^2_{S^{(i)}_{\mathcal{E}}} + \|D^{(i)}_j(\boldsymbol{u}^{(j)}_{\mathcal{E}} - \boldsymbol{u}^{(i)}_{\mathcal{E}})\|^2_{S^{(j)}_{\mathcal{E}}}\right). \quad (6.1)$$

Denote by $\boldsymbol{u}^{(i)}_{\Pi\mathcal{E}}$ and $\boldsymbol{u}^{(j)}_{\Pi\mathcal{E}}$ the restriction to $\mathcal{E}$ of the primal components corresponding to $\boldsymbol{u}^{(i)}_\Gamma$ and $\boldsymbol{u}^{(j)}_\Gamma$. Since $\boldsymbol{u}^{(i)}_{\Pi\mathcal{E}} = \boldsymbol{u}^{(j)}_{\Pi\mathcal{E}}$, we have that

$$\|D^{(j)}_i(\boldsymbol{u}^{(i)}_{\mathcal{E}} - \boldsymbol{u}^{(j)}_{\mathcal{E}})\|^2_{S^{(i)}_{\mathcal{E}}} \le 2\|D^{(j)}_i(\boldsymbol{u}^{(i)}_{\mathcal{E}} - \boldsymbol{u}^{(i)}_{\Pi\mathcal{E}})\|^2_{S^{(i)}_{\mathcal{E}}} + 2\|D^{(j)}_i(\boldsymbol{u}^{(j)}_{\mathcal{E}} - \boldsymbol{u}^{(j)}_{\Pi\mathcal{E}})\|^2_{S^{(i)}_{\mathcal{E}}}.$$

By using the fact that $S^{(i)}_{\mathcal{E}}\left(S^{(i)}_{\mathcal{E}} + S^{(j)}_{\mathcal{E}}\right)^{-1} S^{(j)}_{\mathcal{E}}$ is symmetric and that

$$S^{(i)}_{\mathcal{E}}\left(S^{(i)}_{\mathcal{E}} + S^{(j)}_{\mathcal{E}}\right)^{-1} S^{(j)}_{\mathcal{E}} = \left(S^{(i)^{-1}}_{\mathcal{E}} + S^{(j)^{-1}}_{\mathcal{E}}\right)^{-1},$$

by simple algebra we can deduce that

$$\|D^{(j)}_i(\boldsymbol{u}^{(i)}_{\mathcal{E}} - \boldsymbol{u}^{(i)}_{\Pi\mathcal{E}})\|^2_{S^{(i)}_{\mathcal{E}}} + \|D^{(i)}_j(\boldsymbol{u}^{(i)}_{\mathcal{E}} - \boldsymbol{u}^{(i)}_{\Pi\mathcal{E}})\|^2_{S^{(j)}_{\mathcal{E}}} \le \|\boldsymbol{u}^{(i)}_{\mathcal{E}} - \boldsymbol{u}^{(i)}_{\Pi\mathcal{E}}\|^2_{S^{(i)}_{\mathcal{E}}}.$$

Hence,

$$\|D^{(j)}_i(\boldsymbol{u}^{(i)}_{\mathcal{E}} - \boldsymbol{u}^{(j)}_{\mathcal{E}})\|^2_{S^{(i)}_{\mathcal{E}}} + \|D^{(i)}_j(\boldsymbol{u}^{(j)}_{\mathcal{E}} - \boldsymbol{u}^{(i)}_{\mathcal{E}})\|^2_{S^{(j)}_{\mathcal{E}}} \le 2\|\boldsymbol{u}^{(i)}_{\mathcal{E}} - \boldsymbol{u}^{(i)}_{\Pi\mathcal{E}}\|^2_{S^{(i)}_{\mathcal{E}}} + 2\|\boldsymbol{u}^{(j)}_{\mathcal{E}} - \boldsymbol{u}^{(j)}_{\Pi\mathcal{E}}\|^2_{S^{(j)}_{\mathcal{E}}}. \quad (6.2)$$

Therefore, by combining (6.1), (6.2), and Lemma 5.11, we conclude that

$$\|E_D\boldsymbol{u}_\Gamma\|^2_{\widetilde{S}_\Gamma} \le C|\Xi|\chi^2\left(1 + \log\frac{H}{h}\right)^2 \|\boldsymbol{u}_\Gamma\|^2_{\widetilde{S}_\Gamma},$$

where $|\Xi| = \max_i |\Xi_i|$ and Ξ_i is the set of indices such that Ω_j has a common edge with Ω_i. We conclude the proof of the theorem by using Lemma 6.1. ◻

7. Numerical Results.

Numerical examples are presented in this section to confirm the bound of Theorem 6.2 for different types of subdomains. We use triangular linear Nédélec elements. The first three types are shown in Figure 7.1. Type 1 subdomains have a square geometry, Type 2 subdomains include boundaries with a “sawtooth” shape, and Type 3 subdomains have edges with both straight and fractal segments. We also use Type 4 subdomains, which include small and large squares; see Figure 7.4. We finally consider subdomains obtained by the graph partitioning software METIS; see [18] and Figure 7.6.

Our choices of subdomain geometries are similar to those of [10, Section 5] and [19, Section 5]. For Type 1 and 2 subdomains, the ratio H/h is increased by a a factor of 2 with each additional level of mesh refinement. For Type 3, we divide the unit square into nine squares and construct a fractal edge over each initial edge on the interface. We note that the fractal segment lengths grow by a factor of $4/3$ with each mesh refinement whereas the straight line segments remain constant. For each refinement of Type 3 subdomains, every element edge on the fractal part of the boundary is first divided into three shorter edges of $1/3$ the length. The middle of these edges is then replaced by two other edges with which it form an equilateral triangle. We call the number of partitions realized over the original straight edge the order of the fractal. See Figure 7.2.

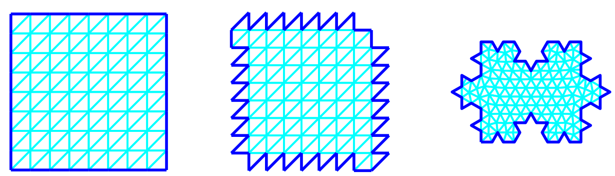

FIG. 7.1. *Subdomains of Type 1, 2 and 3 used in the numerical examples.*

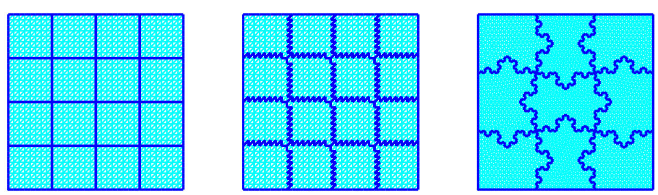

FIG. 7.2. *Domain decomposition used in numerical examples for Type 1, 2 and 3 subdomains.*

To solve the resulting linear systems, we use a preconditioned conjugate gradient method to a relative residual tolerance of 10^{-8} with random right-hand sides. The number of iterations and maximum eigenvalues estimates (in parenthesis) are reported for each of the experiments. The condition number estimates are obtained as in [28, Section 4.4]; see also [30, Section 6.7]. We approximate the condition number by the maximum eigenvalue, since the minimum eigenvalue is always close to 1.

We notice that the numerical experiments for our algorithm show an improvement in the iteration count and the condition number estimates, compared to an iterative substructuring method presented in [11] and a two-level overlapping Schwarz method considered in [4].

EXAMPLE 7.1. *This example is used to confirm the logarithmic factor in the bound of the condition number, for increasing values of H/h, with $N = 16$ subdomains. We note that for Type 2 subdomains with constant coefficients, the condition number is not sensitive to the mesh parameter H/h as shown in Table 7.1. For Type 3 subdomains, we approximate H/h by $\max_i \sqrt{|dof_i|}$; see Table 7.2. We have a growth in the condition number as expected for Type 1 and 3 subdomains; see Figure 7.3.*

TABLE 7.1

Results for the unit square decomposed into 16 subdomains, with $\alpha_i = 1$, $\beta_i = \beta$. I is the number of degrees of freedom on the interface, SE is 24 and 33, for Type 1 and Type 2 subdomains, respectively.

Type	H/h	$\beta = 10^{-3}$	$\beta = 1$	$\beta = 10^3$	I
1	4	9(1.5)	8(1.5)	4(1.1)	96
	8	11(2.1)	11(2.0)	7(1.3)	192
	12	12(2.5)	11(2.4)	8(1.5)	288
	16	13(2.8)	12(2.9)	8(1.7)	384
	24	14(3.4)	14(3.3)	9(2.0)	576
2	4	10(2.0)	10(2.3)	7(1.3)	159
	8	9(1.6)	9(1.6)	8(1.4)	351
	12	9(1.6)	9(1.6)	8(1.4)	543
	16	9(1.7)	9(1.7)	8(1.4)	735
	24	10(1.9)	10(1.9)	8(1.5)	1119

TABLE 7.2

Results for Type 3 subdomains, with $\alpha_i = 1$, $\beta_i = \beta$, $SE = 12$, $N = 9$. Subdomain edges are fractals. TE is the total number of degrees of freedom and I is the number of degrees of freedom on the interface. See Figure 7.3

Order	H/h	$\beta = 10^{-3}$	$\beta = 1$	$\beta = 10^3$	I	TE
2	16	19(1.9)	19 (2.1)	7(1.4)	200	2821
3	26	16(4.3)	16(4.3)	10(2.2)	768	7683
4	44	18(7.3)	19 (7.3)	13(3.7)	3072	21497
5	76	22(9.9)	23(10.2)	15(5.0)	12288	58934

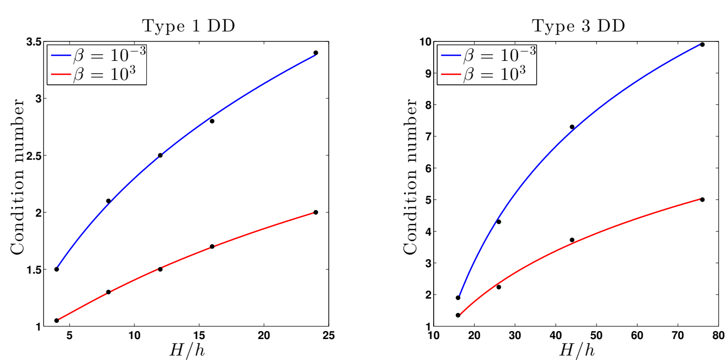

FIG. 7.3. *Least-squares fit to a degree 2 polynomial in* $\log(H/h)$ *for data of Tables 7.1 and 7.2*

EXAMPLE 7.2. *We verify the scalability of our algorithm for Type 1 and 2 subdomains over the unit square. It is clear that the condition number is independent of the number of subdomains, as shown in Table 7.3.*

TABLE 7.3

Results for Type 1 and 2 subdomains, where the unit square is decomposed into N subdomains, with $H/h = 4$, $\alpha_i = 1$ and $\beta_i = \beta$. SE is the number of interior subdomain edges, TE is the total number of degrees of freedom and I the number of degrees of freedom on the interface. Number of iterations and condition number estimates (in parenthesis) are reported for a relative residual tolerance of 10^{-8}.

Type	N	SE	TE	I	$\beta = 10^{-3}$	$\beta = 1$	$\beta = 10^3$
1	64	112	3008	448	9(1.5)	8(1.5)	7(1.3)
	256	480	12160	1920	9(1.5)	9(1.5)	11(1.9)
	576	1104	27456	4416	9(1.5)	9(1.5)	10(1.8)
	1024	1984	48896	7936	9(1.5)	9(1.5)	9(1.6)
2	64	161	3008	735	10(2.0)	11(2.0)	9(1.5)
	256	705	12160	3135	10(2.0)	10(2.0)	12(2.3)
	576	1633	27456	7199	10(2.0)	10(2.0)	15(3.1)
	1024	2945	48896	12927	10(1.9)	10(1.9)	13(2.4)

EXAMPLE 7.3. *This example is used to confirm that the condition number estimate does not require all subdomain edges to be of comparable length. Here, the smaller subdomains shown in Figure 7.4 have only 6 elements, while the mesh parameter H/h is increased for the larger surrounding subdomains. The results are shown in Table 7.4 and Figure 7.5.*

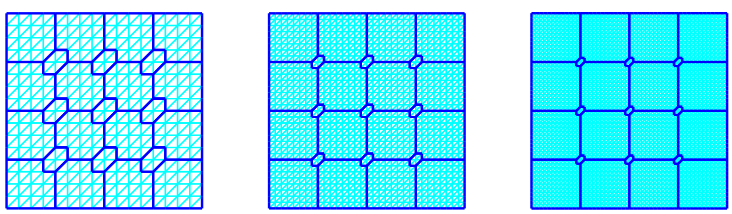

FIG. 7.4. *Domain decomposition used in Example 7.3 for $H/h = 4$, $H/h = 8$ and $H/h = 12$. See also Table 7.4.*

TABLE 7.4

Results for the unit square decomposed into 25 subdomains as shown in Figure 7.4, with $\alpha_i = 1$, $\beta_i = \beta$, $SE = 60$. See also Figure 7.5.

H/h	$\beta = 10^{-3}$	$\beta = 1$	$\beta = 10^3$	I
4	7(1.2)	7(1.2)	5(1.1)	114
8	8(1.4)	9(1.4)	7(1.3)	210
12	8(1.6)	9(1.6)	9(1.7)	306
16	10(1.7)	10(1.7)	10(2.0)	402
20	10(1.8)	10(1.8)	11(2.2)	498

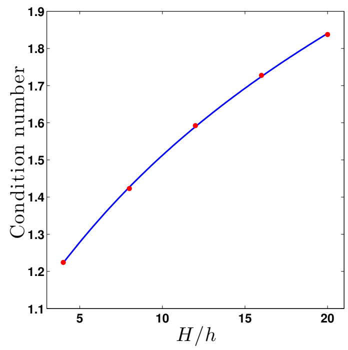

FIG. 7.5. *Least-squares fit to a degree 2 polynomial in* $\log(H/h)$ *for data of Table 7.4. See domain decomposition in Figure 7.4.*

EXAMPLE 7.4. *This example is used to demonstrate that the performance of the algorithm need not diminish significantly when a mesh partitioner is used to decompose the mesh. Example mesh decompositions for $N = 16$ and $N = 64$, shown in Figure 7.6, were obtained using the graph partitioning software METIS, see [18]. Results are shown in Table 7.5.*

TABLE 7.5
Comparison of results for Type 1 subdomains and subdomains generated by METIS. Material properties are homogeneous with $\alpha_i = 1$, $\beta_i = \beta$. For Type 1 subdomains, $H/h = 8$. For subdomains generated by METIS, see Figure 7.6.

Type	N	$\beta = 10^{-3}$	$\beta = 1$	$\beta = 10^3$	I
1	16	11(2.0)	11(2.0)	7(1.2)	192
	64	11(2.1)	11(2.1)	10(1.8)	896
	144	11(2.2)	11(2.1)	12(2.4)	2112
	256	11(2.1)	11(2.1)	14(3.0)	3840
	400	11(2.2)	11(2.1)	14(2.8)	6080
METIS	16	18(8.9)	18(8.8)	9(1.6)	204
	64	27(10.7)	25(10.3)	12(2.3)	963
	144	25(11.7)	25(11.7)	15(2.9)	2258
	256	25(15.0)	25(15.0)	19(4.9)	4061
	400	26(10.6)	26(10.6)	20(6.8)	6420

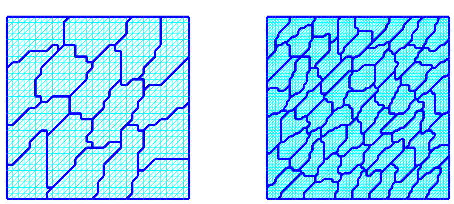

FIG. 7.6. *Decomposition used in Example 7.4, obtained with the software METIS for $N = 16$ and $N = 64$.*

EXAMPLE 7.5. *This example is used to confirm that our estimate is independent of the material property values in each subdomain. Insensitivity to jumps in material properties is* *evident in Table 7.6.*

TABLE 7.6

Results for the unit square decomposed into 9 subdomains. The subdomains along the diagonal have $\alpha_i = \alpha$ and $\beta_i = \beta$, while the remaining subdomains have $\alpha_i = 1$ and $\beta_i = 1$. For Type 1, $H/h = 24$, $I = 288$, $SE = 12$. For Type 2, $H/h = 24$, $I = 560$, $SE = 16$. For Type 3, $H/h \approx 26$, $I = 768$, $SE = 12$ and the fractals segments have order 3.

α	β	Type 1	Type 2	Type 3
10^{-3}	10^{-3}	9(3.0)	8(1.7)	10(3.5)
10^{-3}	1	12(2.9)	9(1.8)	15(3.5)
10^{-3}	10^{3}	10(2.6)	10(2.2)	12(3.6)
1	10^{-3}	9(3.0)	8(1.7)	10(3.5)
1	1	12(3.3)	10(1.8)	16(4.3)
1	10^{3}	10(2.6)	10(2.2)	12(3.7)
10^{3}	10^{-3}	9(3.0)	8(1.7)	10(3.5)
10^{3}	1	12(3.3)	10(1.8)	16(4.3)
10^{3}	10^{3}	10(2.6)	10(2.2)	12(3.7)

EXAMPLE 7.6. *This example is used to compare the behavior of our algorithm when there are discontinuous coefficients inside each substructure. We consider different subdomains with $\alpha_i = 1$ and discontinuous values for β_i. Each subdomain is divided in two sections: in the interior we impose $\beta = 1$ and in the second region $\beta = 10^3$ or $\beta = 10^{-3}$, which is assigned in an "checkerboard" distribution; see Figure 7.7. Results are shown in Table 7.7. We note that our theory does not cover these cases. However, our algorithm works well even though there are discontinuities inside each subdomain.*

TABLE 7.7

Results for the unit square decomposed into 9 subdomains, with $\alpha_i = 1$ and β_i discontinuous inside each subdomain as shown in Figure 7.7.

Type	H/h	$iter(\kappa)$
1	16	10(2.2)
	24	10(2.5)
	36	10(2.9)
2	16	9(2.0)
	24	10(2.2)
	36	10(2.5)
3	16	12(2.6)
	26	12(3.7)
	44	15(6.5)

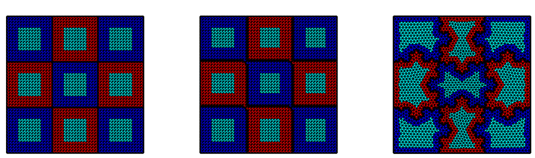

FIG. 7.7. *Coefficient distribution for β used in example 7.6, for Type 1, 2 and 3 subdomains. Elements in blue, cyan and red correspond to $\beta = 10^{-3}$, $\beta = 1$ and $\beta = 10^3$, respectively. See Table 7.7.*

Acknowledgment. The author would like to thank his advisor, Prof. Olof Widlund, for his guidance and suggestions during the work on this article.

REFERENCES

[1] R. Beck, R. Hiptmair, R. H. W. Hoppe, and B. Wohlmuth, *Residual based a posteriori error estimators for eddy current computation*, ESAIM: Math. Model. Numer. Anal., 34 (2000), pp. 159–182.

[2] A. Bossavit, *Discretization of electromagnetic problems: The generalized finite differences approach*, Handb. Numer. Anal., 13 (2005), pp. 105–197.

[3] S. M. Buckley and P. Koskela, *Sobolev-Poincaré implies John*, Math. Res. Lett., 2 (1995), pp. 577–593.

[4] J. G. Calvo, *A two-level overlapping Schwarz method for $H(curl)$ in two dimensions for irregular subdomains*, Tech. Report In progress, Courant Institute, NYU, 2014.

[5] L. Beirão da Veiga, L. F. Pavarivo, S. Scacchi, O.B. Widlund, and S. Zampini, *Isogeometric BDDC preconditioners with deluxe scaling*, Tech. Report TR2013-955, Courant Institute, NYU, 2013. To appear in SIAM J. Sci. Comput.

[6] C. R. Dohrmann, *A preconditioner for substructuring based on constrained energy minimization*, SIAM J. Sci. Comput., 25 (2003), pp. 246–258.

[7] C. R. Dohrmann, A. Klawonn, and O. B. Widlund, *Domain decomposition for less regular subdomains: Overlapping Schwarz in two dimensions*, SIAM J. Numer. Anal., 46 (2008), pp. 2153–2168.

[8] C. R. Dohrmann and J. Mandel, *Convergence of a Balancing Domain Decomposition by Constraints and energy minimization*, Numer. Lin. Alg. Appl., 10 (2003), pp. 639–659.

[9] C. R. Dohrmann, J. Mandel, and R. Tezaur, *An algebraic theory for primal and dual substructuring methods by constraints*, Appl. Numer. Math., 54 (2005), pp. 167–193.

[10] C. R. Dohrmann and O. B. Widlund, *An alternative coarse space for irregular subdomains and an overlapping Schwarz algorithm for scalar elliptic problems in the plane*, SIAM J. Numer. Anal., 50 (2012), pp. 2522–2537.

[11] ———, *An iterative substructuring algorithm for two-dimensional problems in $H(curl)$*, SIAM J. Numer. Anal., 50 (2012), pp. 1004–1028.

[12] ———, *Some Recent Tools and a BDDC Algorithm for 3D Problems in H(curl)*, in Domain Decomposition Methods in Science and Engineering XX, R. Bank, M. Holst, O. B. Widlund, and J. Xu, eds., vol. 91 of Lecture Notes in Computational Science and Engineering, Springer Berlin Heidelberg, 2013, pp. 15–25.

[13] ———, *A BDDC algorithm with deluxe scaling for three-dimensional $H(curl)$ problems*, Tech. Report TR2014-964, Courant Institute, NYU, 2014.

[14] H. Federer and W. H. Fleming, *Normal and integral currents*, Ann. of Math., 72 (1960), pp. 458–520.

[15] R. Hiptmair and A. Toselli, *Overlapping and multilevel Schwarz methods for vector valued elliptic problems in three dimensions*, in Parallel solution of Partial Differential Equations, P. Bjørstad and M. Luskin, eds., vol. 120 of IMA Vol. Math. Appl., Springer, 2000, pp. 181–208.

[16] R. Hiptmair and J. Xu, *Nodal auxiliary space preconditioning in $H(curl)$ and $H(div)$ spaces*, SIAM J. Numer. Anal., 45 (2007), pp. 2483–2509.

[17] P. W. Jones, *Quasiconformal mappings and extendability of functions in Sobolev spaces*, Acta Math., 147 (1981), pp. 71–88.

[18] G. Karypis and V. Kumar, *A fast and high quality multilevel scheme for partitioning irregular graphs*, SIAM J. Sci. Comput., 20 (1998), pp. 359–392.

[19] A. Klawonn, O. Rheinbach, and O. B. Widlund, *An analysis of a FETI-DP algorithm on irregular subdomains in the plane*, SIAM J. Numer. Anal., 46 (2008), pp. 2484–2504.

[20] A. Klawonn and A. Toselli, *A FETI domain decomposicion method for edge element approximations in two dimensions with discontinuous coefficients*, SIAM J. Numer. Anal., 39 (2002), pp. 932–956.

[21] J. H. Lee, *A Balancing Domain Decomposition by Constraints deluxe method for numerically thin Reissner-Mindlin plates approximated with Falk-Tu finite elements*, Tech. Report TR2013-958, Courant Institute, NYU, 2013.

[22] J. Li and O. B. Widlund, *BDDC Algorithms for incompressible Stokes equations*, SIAM J. Numer. Anal., 44 (2006), pp. 2432–2455.

[23] ———, *FETI-DP, BDDC, and block Cholesky methods*, Int. J. Numer. Meth. Engng., 66 (2006), pp. 250–271.

[24] V. G Maz'ja, *Classes of domains and imbedding theorems for functions spaces*, Soviet Math. Dokl., 1 (1960), pp. 882–885.

[25] J.-C. Nédeléc, *Mixed finite elements in* $\mathbb{R}^3$, Numer. Math., 35 (1980), pp. 315–341.

[26] D.-S. Oh, *An overlapping Schwarz algorithm for Raviart-Thomas vector fields with discontinuous coefficients*, SIAM J. Numer. Anal., 51 (2013), pp. 297–321.

[27] D.-S. Oh, C. R. Dohrmann, and O. B. Widlund, *A BDDC algorithm for Raviart-Thomas vector fields*, Tech. Report TR2013-951, Courant Institute, NYU, 2013.

[28] D. O'Leary and O. B. Widlund, *Capacitance matrix methods for the Helmholtz equation on general three-dimensional regions*, Math. Comp., 33 (1979), pp. 849–879.

[29] A. Quarteroni and A. Valli, *Numerical approximation of partial differential equations*, vol. 23 of Springer Ser. Comput. Math., Springer, 2008.

[30] Y. Saad, *Iterative methods for sparse linear systems*, SIAM, 2nd ed., 2003.

[31] A. Toselli, *Overlapping Schwarz methods for Maxwell's equations in three dimensions*, Numer. Math., 86 (2000), pp. 733–752.

[32] ———, *Dual-primal FETI algorithms for edge finite-element approximations in 3D*, IMA J. Numer. Anal., 26 (2006), pp. 96–130.

[33] A. Toselli and X. Vasseur, *Robust and efficient FETI domain decomposition algorithms for edge element approximations*, COMPEL, 24 (2005), pp. 396–407.

[34] A. Toselli and O. B. Widlund, *Domain decomposition methods-algorithms and theory*, vol. 34 of Springer Ser. Comput. Math., Springer, 2005.

[35] A. Toselli, O. B. Widlund, and B. Wohlmuth, *An iterative substructuring method for Raviart–Thomas vector fields in three dimensions*, SIAM J. Numer. Anal., 37 (2000), pp. 1657–1676.

[36] ———, *An iterative substructuring method for Maxwell's equations in two dimensions*, Math. Comp., 70 (2001), pp. 935–949.

[37] O. B. Widlund, *Accommodating irregular subdomains in domain decomposition theory*, in Domain Decomposition Methods in Science and Engineering XVIII, M. Bercovier, M. J. Gander, R. Kornhuber, and O. B. Widlund, eds., vol. 70 of Lecture Notes in Computational Science and Engineering, Springer-Verlag, 2009, pp. 87–98.